Pergamon

Geochimica et Cosmochimica Acta, Vol. 58, No. 18, pp. 3803–3822, 1994

0016-7037/94 $6.00 + .00

0016-7037(94)00176-6

Hydrocarbon biomarkers, thermal maturity, and depositional setting of tasmanite oil shales from Tasmania, Australia

A. T. REVILL,[1] J. K. VOLKMAN,[1] T. O'LEARY,[1] R. E. SUMMONS,[2] C. J. BOREHAM,[2] M. R. BANKS,[3] and K. DENWER[3,*]

[1]CSIRO Division of Oceanography, GPO Box 1538, Hobart, Tasmania 7001, Australia
[2]Australian Geological Survey Organisation, GPO Box 378, Canberra, ACT 2601, Australia
[3]Geology Department, University of Tasmania, GPO Box 252C, Hobart, Tasmania 7001, Australia

(*Received June* 9, 1993; *accepted in revised form March* 18, 1994)

Abstract—This study represents the first geological and organic geochemical investigation of samples of tasmanite oil shale representing different thermal maturities from three separate locations in Tasmania, Australia. The most abundant aliphatic hydrocarbon in the immature oil shale from Latrobe is a C_{19} tricyclic alkane, whereas in the more mature samples from Oonah and Douglas River low molecular weight *n*-alkanes dominate the extractable hydrocarbon distribution. The aromatic hydrocarbons are predominantly derivatives of tricyclic compounds, with 1,2,8-trimethylphenanthrene increasing in relative abundance with increasing maturity. Geological and geochemical evidence suggests that the sediments were deposited in a marine environment of high latitude with associated cold waters and seasonal sea-ice. It is proposed that the organism contributing the bulk of the kerogen, *Tasmanites,* occupied an environmental niche similar to that of modern sea-ice diatoms and that bloom conditions coupled with physical isolation from atmospheric CO_2 led to the distinctive "isotopically heavy" $\delta^{13}C$ values (−13.5‰ to −11.7‰) for the kerogen. $\delta^{13}C$ data from modern sea-ice diatoms (−7‰) supports this hypothesis. Isotopic analysis of *n*-alkanes in the bitumen (−13.5 to −31‰) suggest a multiple source from bacteria and algae. On the other hand, the *n*-alkanes generated from closed-system pyrolysis of the kerogen (−15‰) are mainly derived from the preserved *Tasmanites* biopolymer algaenan. The tricyclic compounds (mean −8‰) both in the bitumen and pyrolysate, have a common precursor. They are consistently enriched in ^{13}C compared with the kerogen and probably have a different source from the *n*-alkanes. The identification of a location where the maturity of the tasmanite oil shale approaches the "oil window" raises the possibility that it may be a viable petroleum source rock.

INTRODUCTION

THE OIL PROSPECTIVITY of onshore Tasmania has long been problematical. Interest in the possibility of finding oil has been stimulated by repeated reports of bitumen strandings on western and southern beaches since the late 19th century (TWELVETREES, 1917). This interest has continued, despite the fact that these coastal bitumens are now thought to arise from Mesozoic or Cainozoic offshore sediments that are poorly represented onshore (VOLKMAN et al., 1992). There have been, however, numerous reports over the last century of oil-seeps onshore (BENDALL et al., 1991), suggesting the possibility that older onshore rocks may also be a source of petroleum. Central to much of this interest has been the organic-rich tasmanite oil shale (subsequently referred to simply as "tasmanite" or "oil shale") which occurs particularly in the north-west of the state (Fig. 1). JAMES et al. (1932) reported that the oil shale was retorted to liberate hydrocarbons as early as 1910, and this carried on until the 1930s, producing about 1.13 megalitres of shale oil.

The tasmanite occurs as a distinctive band low in the Quamby Mudstone. The stratigraphy of Late Palaeozoic sediments in Tasmania has been the centre of much research interest (see CLARKE and FARMER, 1976; CLARKE, 1989) due to the difficulty of applying the (warm water based) internationally accepted biostratigraphic divisions to the cold water environment of Tasmania at this time. Because of this difficulty, the more appropriate Rekunian Series has been proposed (CLARKE and BANKS, 1975; CLARKE and FARMER, 1976) with a subdivision, the Tamarian stage, within which is the Quamby Mudstone (Fig. 2). That part of the Quamby Mudstone containing the oil shale has consistently yielded stage 2 microfloras (TRUSWELL, 1978) and a Faunal Zone 1 macrofauna (Fig. 2; CLARKE and BANKS, 1975). The age has been given as either Early Permian (FOSTER and WATERHOUSE, 1988) or Late Carboniferous (CLARKE, 1992; i.e., a little older or a little younger than 290 my BP, taken as the age of the beginning of the Permian by HARLAND et al., 1990).

The only lithological distinction between the oil shale and surrounding mudstone is that the former contains abundant algal remains. These are dominated by the unicellular alga *Tasmanites punctatus* [NEWTON (1875)] whose biological affinities have been suggested to lie with the extant green alga *Pachysphaera pelagica* [OSTENFELD (1899)] (WALL, 1962). Initially, the tasmanite was thought to have been deposited in an extensive lake (MILLIGAN, 1852), but the discovery of marine fossils (GOULD, 1861) precluded this. Recent work has suggested a nearshore marine origin (BANKS, 1962; CALVER et al., 1984) with the oil shale representing a period of algal blooms (CALVER et al., 1984; CLARKE, 1989). This hypothesis is further supported by comparison of the known occurrence of tasmanite with the inferred palaeogeography of Tasmania during the early Tamarian (BANKS and CLARKE, 1987; Fig. 3).

* *Present address:* RGC Exploration, PO Box 1166, Milton, Queensland 4064, Australia.

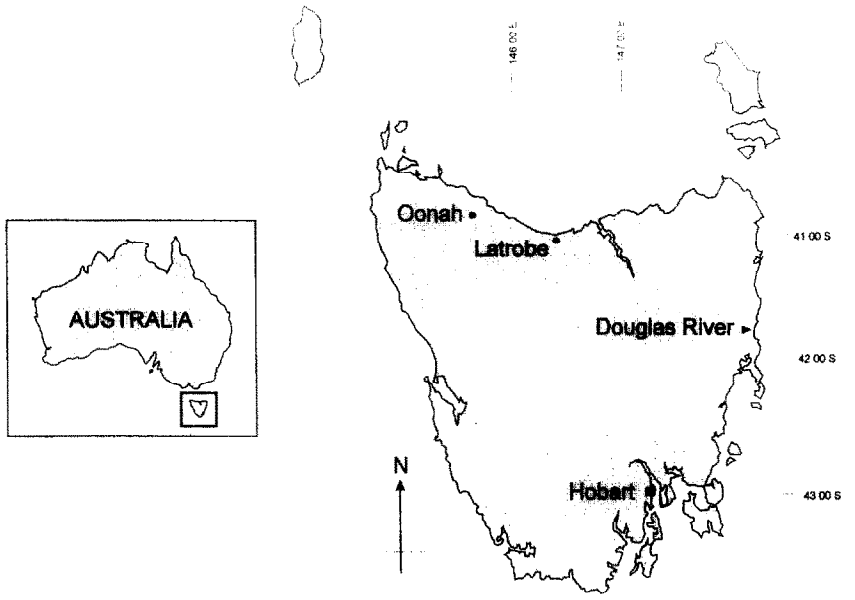

FIG. 1. Sample locations.

There has been much discussion about the correct nomenclature for the abundant microfossils found in the tasmanite (see WALL, 1962). The term spore has been used (SIMONEIT and BURLINGAME, 1973), while studies of some modern prasinophycean genera (*Pachysphaera, Halosphaera,* and *Pterosperma*) have shown that the asexual reproductive cycle consists of a phycoma (cyst) and a motile stage (PARKE and HARTOG-ADAMS, 1965; PARKE, 1966; PARKE et al., 1978). GUY-OHLSON (1988) identified various developmental stages of *Tasmanites* in the Jurassic of Sweden and concluded that the fossil cysts were phycomata. Recent studies (BOALCH and GUY-OHLSON, 1992; GUY-OHLSON and BOALCH, 1992) have indicated that the morphology of fossil *Tasmanites* are sufficiently close to some rarely found living specimens of *Pachysphaera* that the genus *Tasmanites* suffices for both. TAPPAN (1980) indicates that the term phycoma describes the non-motile stage specific to prasinophytes and therefore,

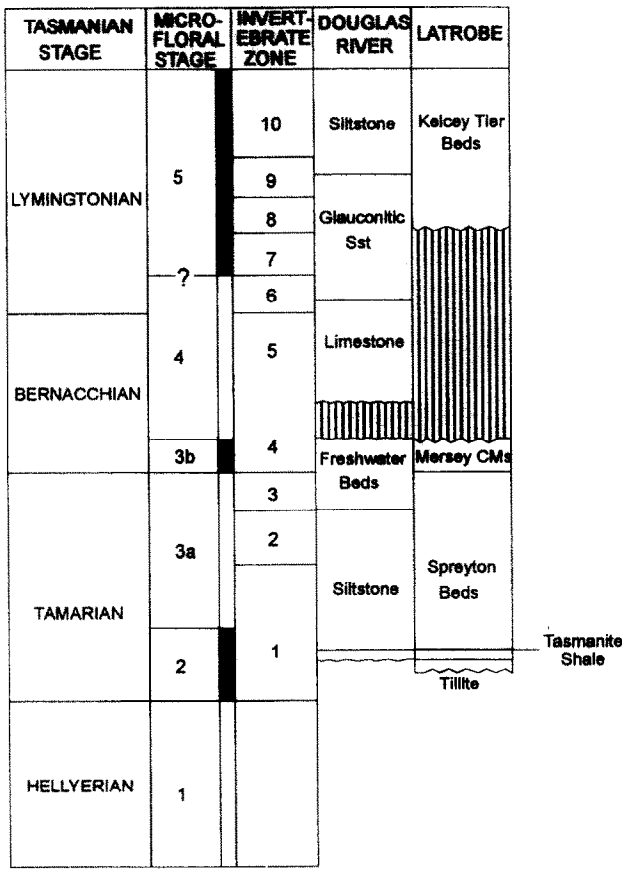

FIG. 2. Correlation chart for the lower (Carboniferous and Permian) sections of the Parmeener Supergroup for Latrobe and Douglas River (adapted from BANKS and CLARKE, 1987). Sst = Sandstone, CMs = Coal Measure Formation.

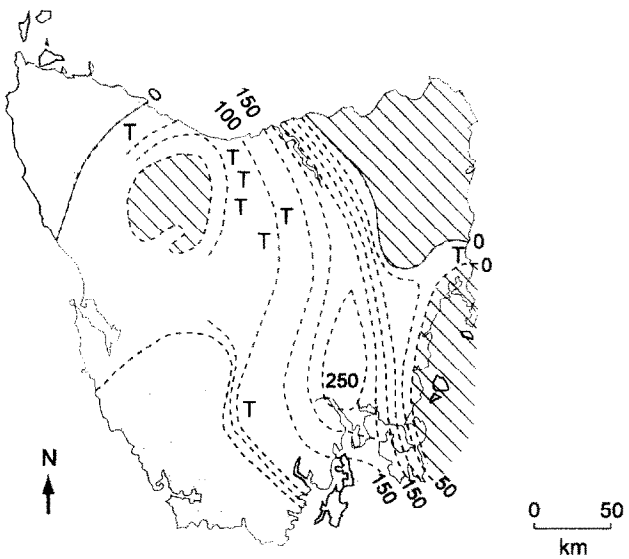

FIG. 3. Suggested paleogeography of Tasmania during the Early Tamarian stage. Dashed lines = isopachs, numbers = thicknesses in metres, T = occurrence of tasmanite oil shale, ▨ = land areas, □ = areas of unknown geography. (Adapted from BANKS and CLARKE, 1987).

to use this description would indicate an acceptance that *Tasmanites punctatus*, found in Tasmanian tasmanite, is the equivalent of a modern prasinophyte. To avoid any taxonomic inference, the abundant microfossils in these samples will be referred to as *Tasmanites* or simply fossils. Although known to range from the Cambrian (540 Ma) to present, *Tasmanites* and related forms occur in high concentrations only in the tasmanite deposits of Tasmania (Permian) and Alaska (Jurassic) with other less abundant occurrences in the Sahara and Brazil (AQUINO NETO et al., 1992).

The fossils were spheroidal, but become disc shaped with sediment compaction, ranging in size from <0.1 to >0.6 mm in diameter. The wall of the fossil is formed of two to three layers, with the outer layer rarely preserved. The middle layer forms the bulk of the wall, the inner layer being thin and fibrous (KANTSLER, 1980).

The algal origin for the tasmanite and its organic richness has led to a wide range of geochemical studies of the kerogen. Data have been presented on carboxylic acids (BURLINGAME et al., 1969; SIMONEIT and BURLINGAME, 1973), and more recently the hydrocarbon content (PHILP et al., 1982; AZEVEDO et al., 1990; SIMONEIT et al., 1990; AZEVEDO et al., 1992). These studies have identified novel aliphatic and aromatic compounds, but all have been based on samples from the one site at Latrobe (Fig. 1), where the oil shale is relatively immature. In this paper we report a comprehensive organic geochemical study of the tasmanite oil shale, including a comparison of immature and mature samples from different locations in Tasmania.

EXPERIMENTAL

Samples

Samples were collected from rock outcrops at Oonah, Latrobe, in the Mersey Valley and from a core taken at Douglas River (Fig. 1; for stratigraphy see Fig. 2). The rock sample from Latrobe shared many of the characteristics of that from Oonah, except that it came from a continuous 1.8 m seam, 21.4 m above the basal conglomerate within the Spreyton beds (Fig. 2). A spore concentrate was obtained from a sample collected at Oonah by density separation of the fossils from the crushed rock using ferric chloride.

Extraction

Total solvent-extractable compounds were obtained by sonication of the crushed rock samples (ca. 50 g) with chloroform/methanol (2:1, 3 × 50 mL). The composition of a portion of the total extracts was determined either by gravimetry after fractionation or by Iatroscan thin-layer chromatography-flame ionisation detection, using hexane as the developing solvent (VOLKMAN et al., 1986). Saturated and aromatic hydrocarbons were isolated by applying 30 mg of extract to a glass column containing 3 g of silicic acid (100–200 mesh) capped with 1 g of activated alumina (BDH). Aliphatic hydrocarbons were eluted with hexane (20 mL) and a second fraction containing aromatic hydrocarbons was obtained by eluting with hexane:toluene (1:1; 20 mL). Resins and asphaltenes were eluted with chloroform (20 mL) and methanol (10 mL).

Analyses

Hydrocarbon fractions were analysed by capillary gas chromatography on a 50 m nonpolar methyl silicone fused silica capillary column (HP-1, 0.32 mm i.d., 0.25 μm film) with on-column injection and hydrogen as the carrier gas. The temperature program was 45°C for 1 min, followed by a ramp to 120°C at 30°C min^{-1} then a ramp to 310°C at 4°C min^{-1}. The oven was then maintained isothermally for 15 min.

Biomarker information was obtained by gas chromatography-quadrupole mass spectrometry (Hewlett Packard 5790 MSD with HP 5890 GC and 59970A computer workstation) in selected ion monitoring (SIM) mode. Typical conditions were: electron multiplier 2200 V, transfer line 310°C, electron impact energy 70 eV. GC conditions were as above except that helium was used as carrier gas. Samples were also analysed using metastable reaction monitoring GC-MS using a VG 70E instrument fitted with an HP 5790 GC and controlled by a VG 11-250 data system. The GC was equipped with a HP Ultra-1 capillary column (50 m × 0.2 mm i.d.) connected to a OCI-3 cooled on-column injector (SGE) with a retention gap of uncoated fused silica (0.5 m × 0.33 mm i.d.). The oven was programmed from 50 to 150°C at 10°C min^{-1} and then to 300°C at 3°C min^{-1} with a final hold time of 30 min. The carrier gas was hydrogen with a linear flow of 30 cm s^{-1}. The mass spectrometer was operated with a source temperature of 240°C, ionisation energy of 70 eV and interface and re-entrant at 310°C. In full scan mode the MS was operated from *m/z* 650 to *m/z* 50 at 1.8 s per decade and an inter-scan delay of 0.2 s. In MRM mode, the magnet current and ESA voltage were switched to sequentially sample 26 selected parent-daughter pairs. The sampling time was 40 ms per reaction with a 10 ms delay giving a total cycle time of 1.3 s.

Gas chromatography-isotope ratio mass spectrometry (GC-IRMS) was carried out as described by HAYES et al. (1990) using a Finnigan-MAT 252 isotope ratio mass spectrometer linked to a Varian 3400 GC via a cupric oxide combustion furnace operated at 900°C. Isotopic calibration was made using an external primary CO_2 standard introduced via a sample bellows and change-over valve and checked using deuterium labelled *n*-alkanes as internal standards. The latter, in hexane, were co-injected with the sample onto a J&W DB-5 capillary column (30 m × 0.25 mm i.d.) using a Varian SPI injector. The oven was programmed from 50–300°C at 6°C min^{-1}.

Closed-System Pyrolysis

Kerogen was isolated from the tasmanite shale by standard acid digestion techniques and pyrolysed in evacuated quartz tubes for 72 h at 300, 330, and 350°C, in the presence of water. Only liquid products were isolated and these were treated in the same way as other extracts. Rock-Eval derived kinetic parameters on whole rock samples of Latrobe tasmanite (AGSO #1995) were determined by Daniel Jarvie, Humble Instruments, Humble, Texas.

RESULTS AND DISCUSSION

Geological Setting of the Tasmanite Oil Shale

The tasmanite at Oonah consists of two seams, separated by up to 6.7 m of siltstone. The lower and upper seams contain two and three *Tasmanites*-rich beds, respectively. These beds consist of a multiplicity of lenses, each up to about a millimetre thick and a few centimetres long, separated by silt layers. The beds generally show a gradually increasing concentration of algal remains upwards. The fossil content decreases rapidly at the top of each bed. The oil shale contains fossils in spherical or flattened forms, the latter being much more common. Spherical *Tasmanites* are observed in fossil-poor sediment, but are absent or rare in fossil-rich sediment (Table 1), and tend to be filled with framboidal pyrite with or without collophane. The flattened disks are probably produced by compaction of the spheroidal form. The fossils exist as thin- and thick-walled specimens, the latter having two distinct walls (Fig. 4). The samples from Oonah contain relatively high levels of clay and silt (quartz) grade sediments. The fossil-rich sediments also contain a greater abundance of elongate, horizontal, silica-filled burrows (Table 1).

Table 1. Examples of oil shale characteristics at Oonah.

	Lower bed-lower seam	Lower bed - Upper seam	Middle bed - Upper seam	Upper bed - Lower seam
Thickness of oil shale (m)	0.28-0.42	0.3-0.7	0.38-0.59	0.24-0.28
Thin walled : thick walled fossils	16:1	6.5:1	10.5:1	5.6:1
% Matrix	48.9	71.4	48.8	74.8
% Fossils	36.5	10.1	32.2	5.4
% Spherical fossils	<0.2	0.4	0.2	0.6
% Pyrite framboids	3.5	2.0	4.3	3.7
% Non-framboidal pyrite	1.3	<0.2	<0.2	<0.2
% Vitrinite	0.5	0.2	0.4	n/d
% Elongate burrows	1.2	0.6	1.4	0.6
% Other*	7.9	15.5	12.5	15.3

* Predominantly clay and silt
n/d = not detected
Percentages are from point counts using approximately 500 data points

In the sample from Latrobe, silica-filled burrows are less prevalent and smaller than in the sediments from Oonah. The oil shale at this site exhibits large-scale lensing as well as the small-scale lensing noted above. This suggests a fluctuating environment, and the oil shale maintains a constant thickness possibly indicating an almost flat sea floor.

Within the core taken from Douglas River, two beds of oil shale can be recognised between 320 and 321.5 m (CALVER et al., 1984). The lower bed exhibits a fossil morphology very similar to that from Latrobe. The upper bed has a thin (20 cm thick) basal conglomerate which fines upwards into the oil shale. Similar small-scale structures to those in the sample from Latrobe can be observed and the top of the shale is characterised by flame structures. The oil shale is overlain by a thin fining upwards sequence (ca. 50 cm thick) commencing with conglomerate. Dispersed *Tasmanites* are observed in the silt at the top of this sequence.

Bulk Parameters

Bulk parameters are given in Table 2. The samples from Oonah represent a span from the upper tasmanite seam to below the lower seam.

Total organic carbon (TOC) concentrations are consistently greater in the immature sample from Latrobe and the more mature Douglas River sample than in that of intermediate thermal maturity from Oonah (Table 2). There appears to be no direct correlation between organic carbon content and sulphur concentration in the Oonah sediments, except possibly in the upper seam (Fig. 5). The majority of sulphur is framboidal (Table 1) with the greatest concentration coinciding with the fossil-rich sediments. In the sample from Latrobe, pyrite is present in lower concentrations than at Oonah and appears to be proportional to the TOC content (Fig. 5). Despite having the lowest maturity, the relative amount of extractable organic matter in the Latrobe material is ca. three times that of the other samples. This probably reflects a generally higher fossil concentration in these samples, with some being almost 74% *Tasmanites*.

Total extractable organic matter contained from 56% hydrocarbons in the Latrobe sample to 95% hydrocarbons in the lower shale seam at Oonah; the remainder being attributed to polar material (Table 2).

The high Hydrogen Index (HI) of the Latrobe, Oonah, upper seam and Douglas River samples (Table 2) classify the kerogen as containing hydrogen-rich Type I organic matter (TISSOT and WELTE, 1984) wherein over 70% of the organic

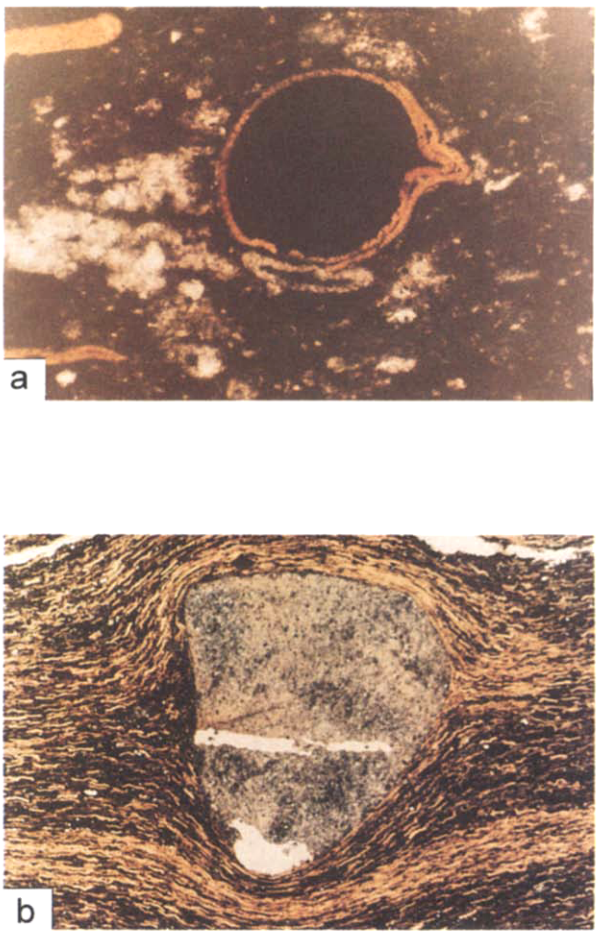

FIG. 4. (a) Fossil *Tasmanites* filled with pyrite from Oonah (diameter = ca. 0.5 mm). (b) Dropstone in tasmanite shale from Oonah. Note how the stone breaks the bedding of the shale, (magnification = ×10).

Table 2. Bulk parameters for tasmanite samples

Sample	Sample No.†	TOC (% whole sample)	EOM (mg/g TOC)	Iatroscan TLC-FID		Rock-Eval						
				Hydrocarbons (%, (mg/g TOC))	Polars (%)	T_{max} (°C)	S_1 (kg/Tonne)	S_2 (kg/Tonne)	S_3 (kg/Tonne)	PI	HI	OI
Latrobe	1	31.3	52	56* (29)	44	444	12.5	304.2	5.6	0.039	972	18
Oonah												
Upper Seam												
Total	2	6.9	66	94 (62)	6	443	3.6	65.2	0.3	0.052	937	4
fossil Concentrate	3	63.0	23	85 (19)	15	446	30.8	590.8	2.3	0.050	937	3
Siltstone above seam	9	1.01	n.m.	n.m.	n.m.	437	0.04	0.89	0.73	0.04	88	72
Siltstone between seams	7	0.78	n.m.	n.m.	n.m.	440	0.07	1.30	0.34	0.05	166	43
Lower Seam												
Total	6	8.1	32	95 (30)	5	440	1.4	54.4	2.2	0.025	675	27
fossil Concentrate	4	61.3	n.m.	n.m.	n.m.	444	22.82	534.94	3.23	0.04	872	5
Siltstone below seam	8	1.1	35	73 (25)	27	436	0.1	1.8	0.6	0.052	163	51
Douglas River	5	17	34	90 (31)	10	446	6.3	147.5	0.2	0.041	868	1

† Sample number refers to Fig. 13
n.m. = not measured
* determined by gravimetry
PI = Production Index = $S_1 / S_1 + S_2$

matter is convertible to hydrocarbons. The slightly reduced HI value from the Oonah lower seam may be a result of more oxidation/reworking consistent with the elevated Oxygen Index (OI) value.

Hydrocarbon Distributions and Source Characteristics

The GC-FID traces (Fig. 6) of the saturated hydrocarbons from the tasmanite extracts show *n*-alkane distributions dominated by lower molecular weight components with distributions maximising between *n*-C_{11} and *n*-C_{13}, with little odd or even predominance (Table 3). Samples also contained significant amounts of the acyclic isoprenoids pristane and phytane, though in different relative proportions (Table 3). The siltstone sample has a Pr/Ph ratio higher than the oil shales (Table 3), consistent with deposition under more oxic conditions.

For the purposes of this study, detailed analyses were only conducted on three of the samples: a thermally immature rock sample from Latrobe, the *Tasmanites* fossil concentrate from Oonah, and the core sample from Douglas River. All the samples contain steranes and diasteranes as shown by the *m/z* 217 mass chromatograms (Fig. 7), which is in contrast to their presence as only "trace components" in a sample from Latrobe (Fig. 1) analysed by SIMONEIT et al. (1990).

The relative proportions of C_{27}, C_{28}, and C_{29} steranes show some variation between the samples (Table 3) with C_{29} dominant in the Latrobe sample, C_{27} in Oonah and no preference at Douglas River. Although this may reflect subtle differences in source inputs, maturity will also have an influence. C_{30} 24-*n*-propylcholestanes which are generally accepted to be indicative of a marine source (MOLDOWAN et al., 1990) could not be easily detected in the *m/z* 217 mass chromatogram, but were readily identified (though less so in the Douglas River sample) using MRM together with 2α-methyl and 3β-methyl sterane isomers (Figs. 8–10). The samples also contain relatively high proportions of diasteranes (Fig. 7; Table 3) which were not reported in samples previously analysed (SIMONEIT et al., 1990).

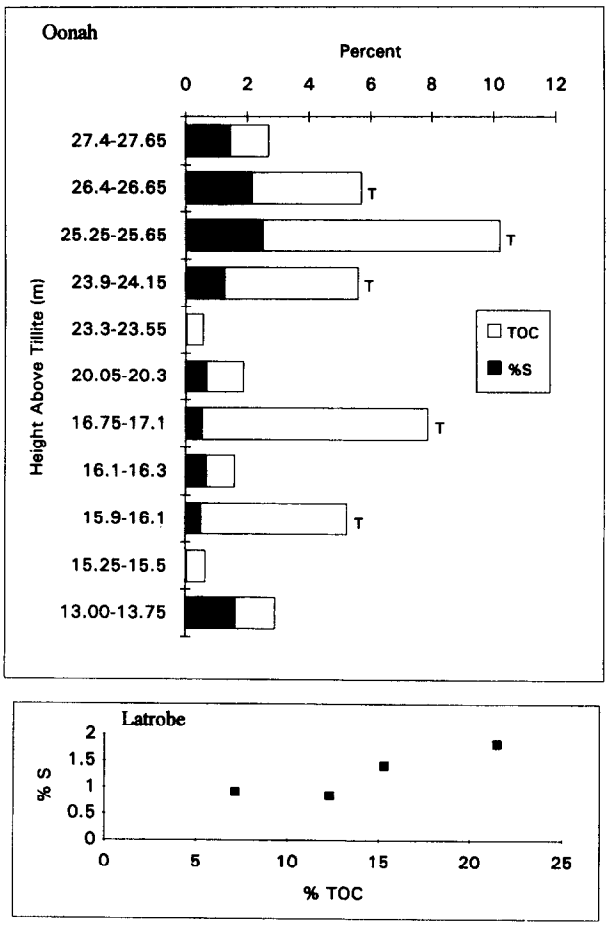

FIG. 5. Relationship between TOC and sulphur content in tasmanite samples. The upper graph shows the relationship with height above the Wynard tillite in a sample from Oonah. T indicates the oil shale seams. The lower graph shows the general relationship in samples taken from Latrobe.

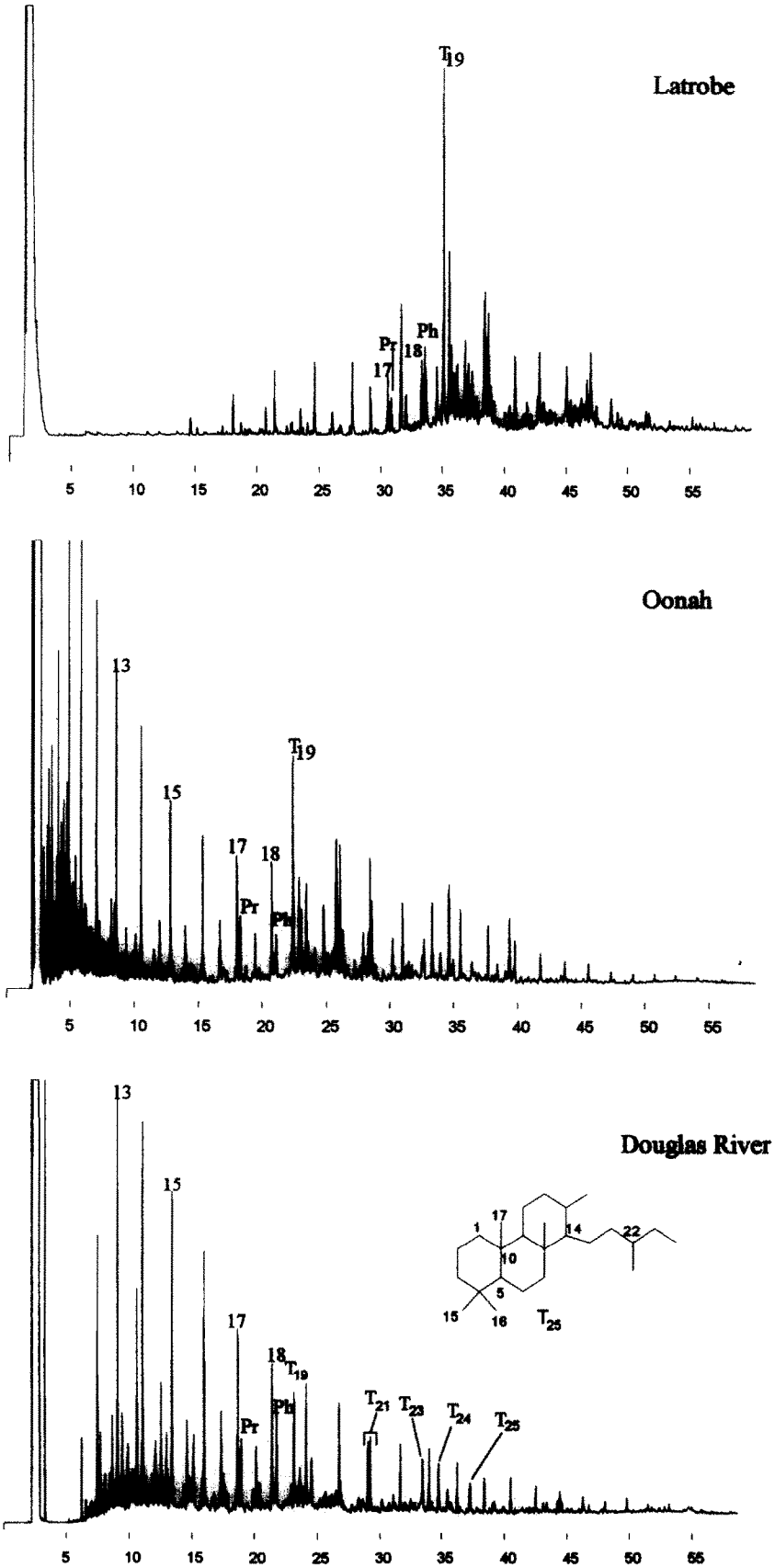

FIG. 6. Gas chromatograms of the aliphatic fractions of extracts from samples taken from Latrobe, Oonah, and Douglas River and an example tricyclic (cheilanthane) structure. Numbers refer to carbon number; Pr = pristane; Ph = phytane; T = tricyclic alkane. Note that the Latrobe fraction was analysed using a different temperature program.

Table 3: Molecular data for tasmanite samples

Sample	Parameter 1 Pr/Ph	2 Pr/C_{17}	3 CPI	4* steranes $C_{27:28:29}$	5* Diasteranes	6* 20S/S+R	7* αββ/αββ + ααα	8 MPI
Latrobe	0.45	0.62	n.d.	1.4:1:2.6	0.12	0.11	n.d.†	n.d.‡
Oonah								
Upper Seam								
Total	1.6	0.69	0.92	n.m.	n.m.	0.30	0.15	n.m.
fossil concentrate	1.5	0.60	1.03	2.2:1:1.9	0.35	0.35	0.15	0.46
Lower Seam								
Total	1.4	0.48	0.83	n.m.	n.m.	0.31	n.m.	n.m.
Siltstone	3.1	0.91	1.40	n.m.	n.m.	n.m.	n.m.	n.m.
Douglas River	0.7	0.45	0.98	2:1:2	0.64	0.54	0.5	0.36

* calculated from MRM data, † αββ probably absent, isomer is 20R 5β,14α,17α(H), .‡ MPI not applicable at this maturity
n.d. = Not detected; n.m. = Not measured
Parameters:
1. Pristane / Phytane
2. Pristane / *n*-C_{17}
3. Carbon Preference Index $= \frac{(\%C_{23} - C_{33}\text{ odd}) + (\%C_{23} - C_{31}\text{ odd})}{2(\%C_{24} - C_{32}\text{ even})}$
4. 5α,14α,17α(H) 20R steranes
5. C_{29} Diasteranes (βα 20S + 20R) / (ααα + αββ 20S & 20R)
6. C_{29} ααα sterane 20S / (20S + 20R)
7. C_{29} αββ 20R steranes / C_{29} 20R (ααα +αββ) steranes
8. Methyl Phenanthrene Index $= \frac{1.5(2\text{-}MP + 3\text{-}MP)}{P + 1\text{-}MP + 9\text{-}MP}$

The GC-FID chromatograms and extended *m/z* 191 mass chromatograms for each sample show a high abundance of tricyclic compounds (Figs. 6, 11) and these extend to at least C_{35}. In the *m/z* 191 chromatograms hopanes occur in trace amounts while C_{21}, C_{23}, and C_{24} tricyclic compounds show the greatest intensity. However, the FID chromatogram reveals the predominant tricyclic terpane is a C_{19} compound. In the C_{19} pseudo homologue, the abundance of the *m/z* 191 ion is minor compared with the base peak at *m/z* 123 (AQUINO NETO et al., 1982). In the MRM reactions used to detect hopanes (Figs. 8–10; e.g., 412 → 191 for the C_{30} hopane), tricyclic terpanes appear as nonquantitative artefacts as a consequence of their high relative abundance and the limitations of the linked scan technique used for the analysis. Only the C_{30} tricyclic is specifically detected using the 416 → 191 reaction. Measurement of the C_{27} Ts/Tm hopane ratios was not possible due to interference from an unknown compound co-eluting with Ts.

Examination of the aromatic fraction of samples from Oonah and Douglas River show they are dominated by a single compound (Fig. 12) which was identified by GC-MS as a C_3-phenanthrene. This was positively identified by co-injection with an authentic standard as 1,2,8-trimethylphenanthrene. This compound is seen as one endmember of an identifiable aromatisation sequence as indicated by the presence of partially aromatized intermediates in the less mature samples from Latrobe (Fig. 12; Scheme 1).

Maturity

The samples from Latrobe and the *Tasmanites* concentrate from Oonah exhibit a predominance of the thermodynamically less stable 5α,14α,17α(H) (cf. 5α,14β,17β(H)) sterane isomers (Table 3) indicating that they are thermally immature. This is further emphasised by the greater proportion of the 5α,14α,17α(H) 20R epimer compared with the 20S epimer and the presence of small amounts of 5β(H)-steranes (as determined by metastable reaction monitoring, MRM). A value of 0.54 for the 20 S/S + R sterane ratio (Table 3) suggests the Douglas River sample is within the oil window (PETERS and MOLDOWAN, 1993). An *αββ-ααα* ratio of 0.5 is consistent with this, the onset of the oil window occurring at about 0.25 (PETERS and MOLDOWAN, 1993).

Maturity estimates based on phenanthrenes (namely the methylphenanthrene index, MPI; Table 3) showed little discrimination. The uniformity in the MPI has been observed previously for low maturity and hydrogen-rich marine organic matter (RADKE et al., 1986; BOREHAM et al., 1988). The presence of aromatic compounds which appear to be derived from the tricyclic precursors in such immature samples (both this study, AZEVEDO et al., 1992, and REVILL et al., 1993) suggests that aromatisation has occurred early in the maturation process. This possibly reflects the unusual nature of the organic matter or microbial influences on the aromatisation processes (TRENDEL, 1985; LOHMANN, 1988; TRENDEL et al., 1989; WOLFF et al., 1989).

There is little evidence to suggest which tricyclic compound is being preferentially converted to the aromatic compounds. The only noticeable correlation being a relative decrease in the complexity of the *m/z* 191 mass chromatogram in the C_{20} region in the Douglas River sample compared with the Oonah *Tasmanites* concentrate (Fig. 11), which is assumed to be a maturity driven decrease in the three stereoisomers relative to the 13β(H),14α(H) compound (CHICARELLI et al., 1988).

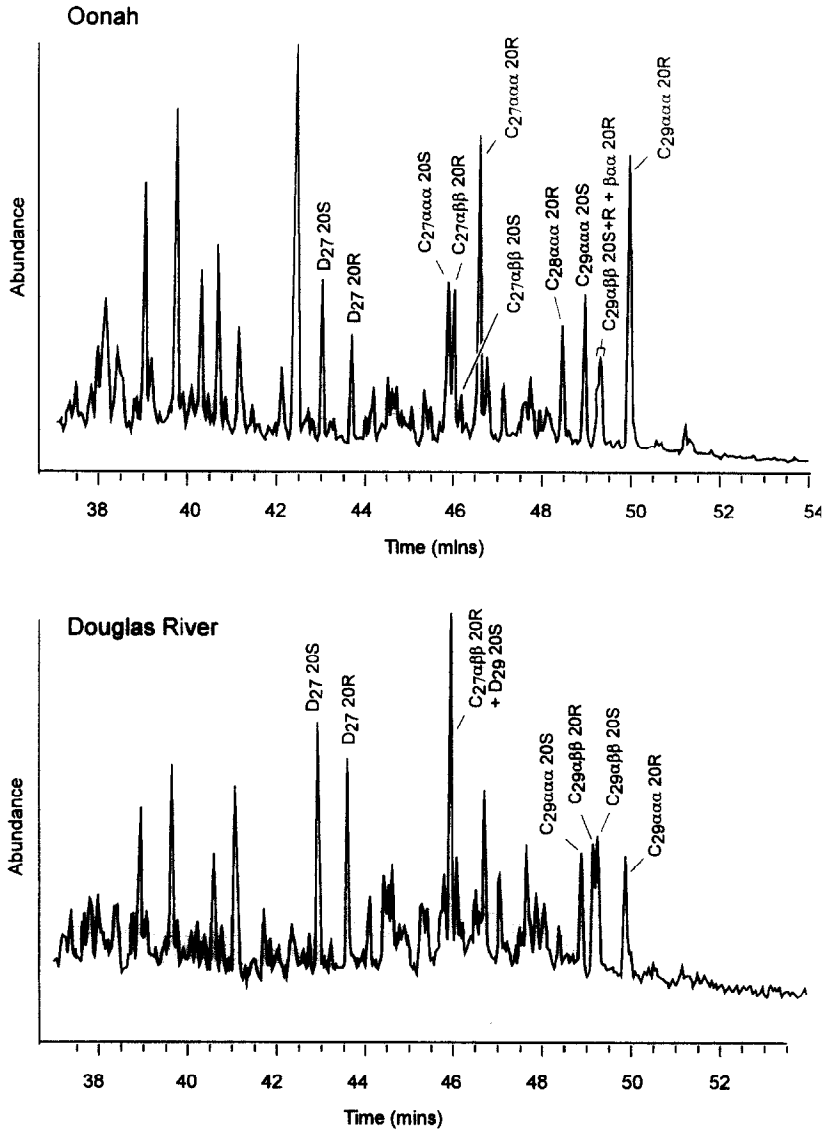

FIG. 7. Extended m/z 217 mass chromatograms for samples from Oonah and Douglas River. Numbers refer to carbon number; D = diasteranes; 20S and 20R refer to stereochemistry at carbon 20. Those denoted $\alpha\alpha\alpha$ 20R have the biological stereochemistry, i.e., 5α,14α,17α(H)-20R with the other signals arising from "geological" isomers.

The plot of T_{max} vs. HI (Fig. 13) shows very similar T_{max} (443–446°C) values for the Latrobe, Oonah fossil concentrate and Douglas River samples. However, the siltstone from above and below the oil shale has a similar maturity but shows a much lower T_{max} (436°C), equivalent to a vitrinite reflectance of 0.5% for Type III kerogen (Fig. 13). This emphasises the limited use of the T_{max} parameter in assessing the thermal maturity of Type I kerogens (TISSOT et al., 1987).

The Production Index (PI) for the most thermally mature sample (Douglas River) is only 0.04 (4%; Table 2), which indicates an immature kerogen (BORDENAVE et al., 1993). This suggests that the biomarker data (steranes) are overestimating the thermal maturity of the samples, which is consistent with recent results. MARZI and RULLKÖTTER (1992) calculated an activation energy for sterane isomerization at C_{20} of 169 kJ/mol, while kinetic data derived for the tasmanite indicates a typical Type I distribution (TISSOT et al., 1987). There is a very narrow distribution of activation energies for kerogen transformation (Fig. 14) which, in combination with the frequency factor of 8.9×10^{13} s^{-1}, indicates a relatively labile kerogen once generation commences. When these data are used to model maturity it becomes clear that the 20 S/20 R isomerisation is complete before the onset of significant hydrocarbon generation (Fig. 15). In contrast, the kinetic data for sterane isomerisation calculated by MACKENZIE and MCKENZIE (1983) predicts over 50% kerogen conversion for the Douglas River sample (Fig. 15), clearly inconsistent with its high HI value.

Calculation of the Transformation Ratio (TR), according to hydrogen index (HI) values

$$TR = \frac{HI_0 - HI_z}{HI_0}$$

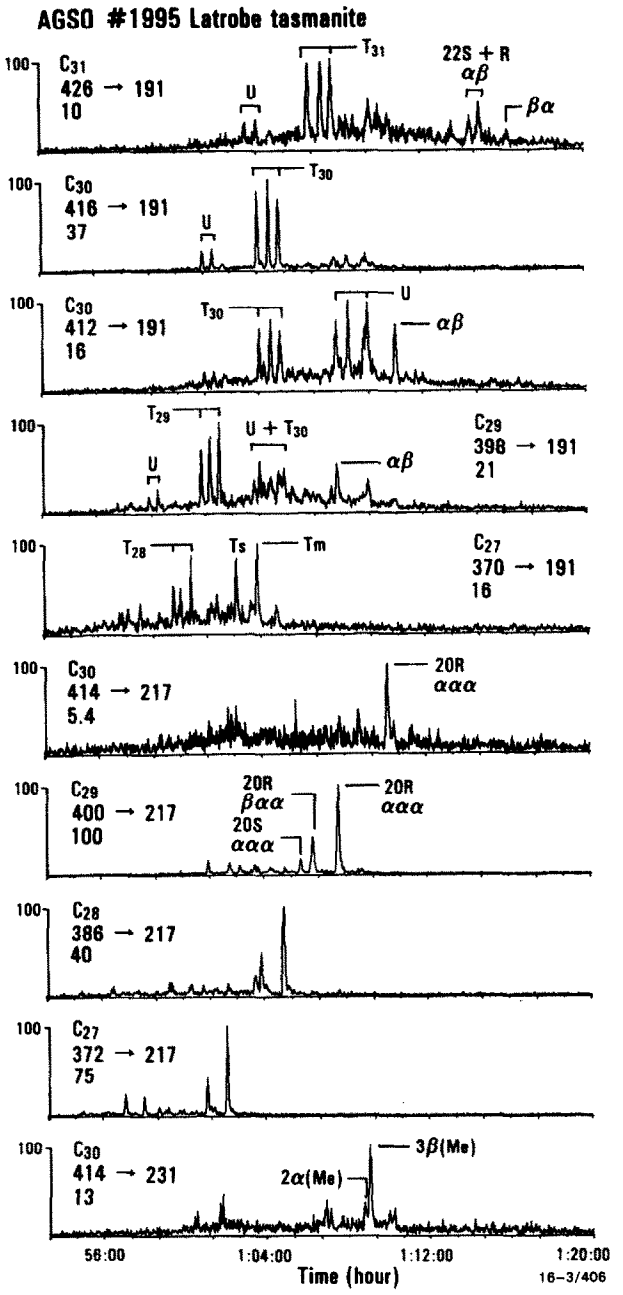

FIG. 8. Distribution of sterane and terpane biomarkers in the saturated hydrocarbon fraction isolated from the Latrobe sample. The data were acquired by gas chromatography–mass spectrometry using metastable reaction monitoring (MRM). Each trace is identified with the carbon number, the reaction as determined by the masses of the parent and daughter ions, and a normalised relative abundance. The last peak to elute in each sterane trace (i.e., those denoted $\alpha\alpha\alpha$-20R) have $5\alpha,14\alpha,17\alpha$(H)-20R stereochemistry with the other signals arising from "geological" isomers. The desmethyl steranes are 24-*n*-propylcholestane (C_{30}), 24-ethylcholestane (C_{29}), 24-methylcholestane (C_{28}), and cholestane (C_{27}). The C_{30} methylsteranes are 24-ethylcholestanes with an additional methyl group in ring-A, i.e., 2α-methyl and 3β-methyl which are denoted 2α(Me), 3β(Me), respectively. Hopanes are denoted H, tricyclics T, and unknown compounds U. Tricyclic terpenoids appear in each hopane reaction as artefacts of the MRM analysis using the linked scan technique. For example, T_{30} is specifically detected in the 416 → 191 reaction. It also appears as an artefact, along with T_{31} in the 412 → 191 reaction.

(where HI_0 and HI_z are the initial HI value and the HI at a depth z, respectively, and HI_0 is taken as the value for Latrobe; Table 2), shows the Douglas River sample to have a TR value of 0.1, considered to define the onset of petroleum generation. Thus, from the kinetic data curve (Fig. 14) it is clear that this sample has only just started hydrocarbon production, but significantly, an increase of only 10–15°C to exceed the activation energy would see a rapid increase in the amount of petroleum production. The production curve (Fig. 15) shows that some hydrocarbons have been produced quite early in the maturation sequence, and this is probably

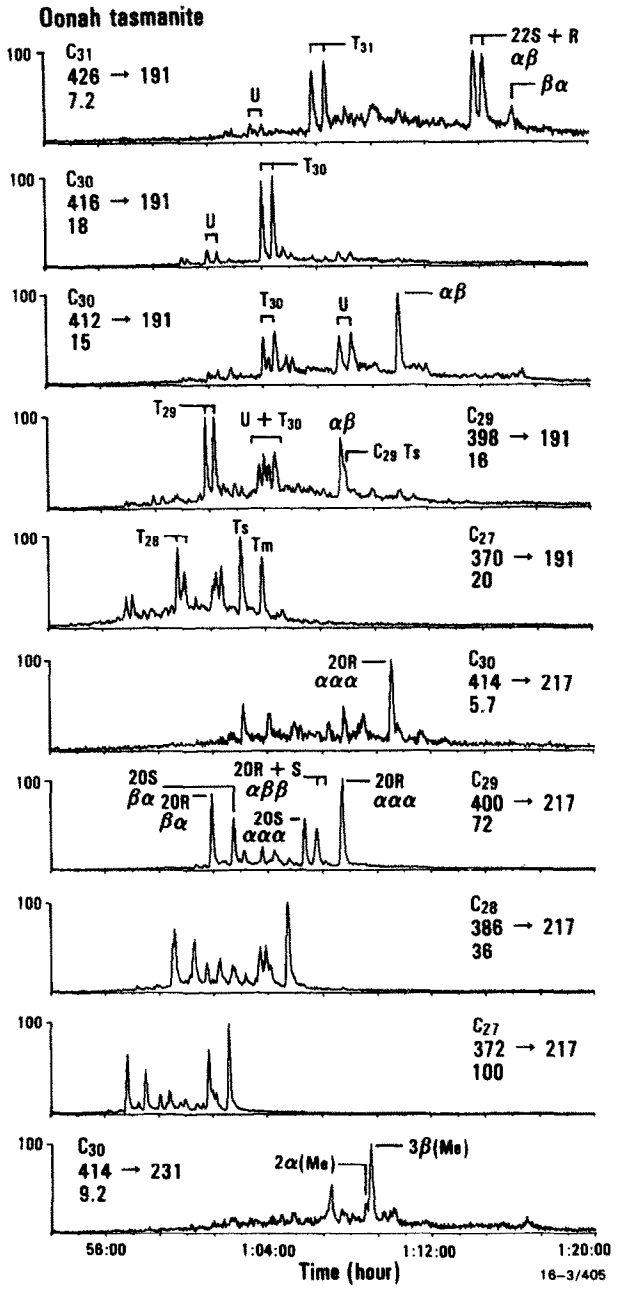

FIG. 9. Distribution of sterane and terpane biomarkers in the saturated hydrocarbon fraction isolated from the Oonah sample, from GC-MS analysis with MRM (see Fig. 8 legend for an explanation of symbols).

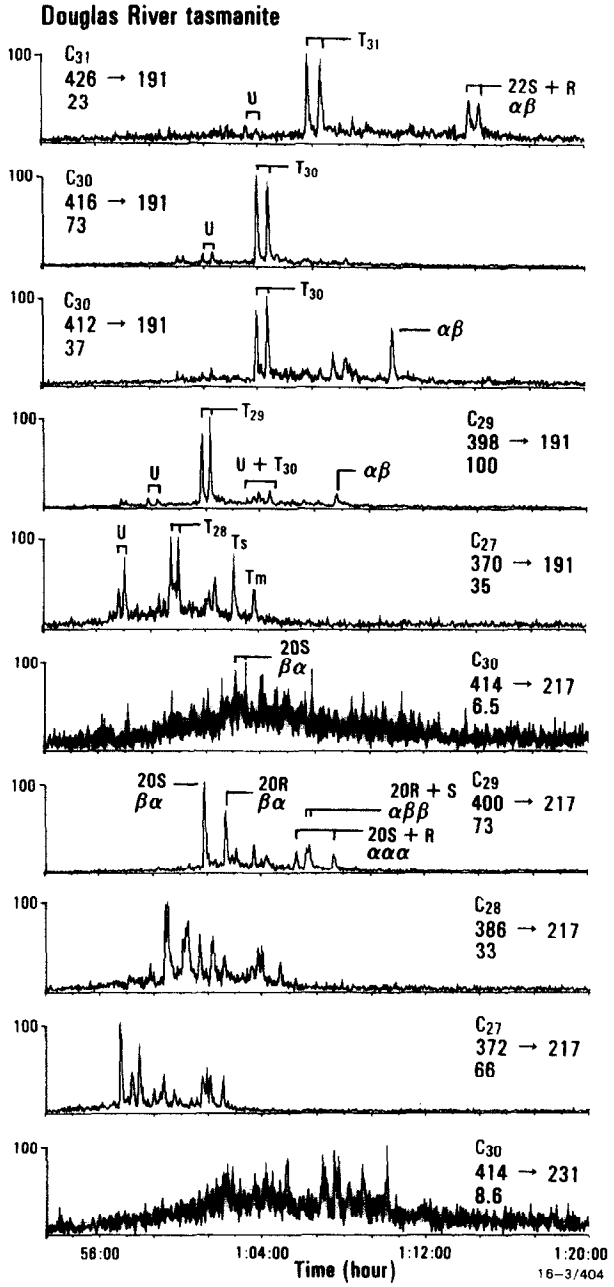

FIG. 10. Distribution of sterane and terpane biomarkers in the saturated hydrocarbon fraction isolated from the Douglas River sample, from GC-MS analysis with MRM (see Fig. 8 legend for an explanation of symbols).

due to the presence of weaker bonds within the kerogen. These are represented by the lower activation energies (205 and 209 kJ/mol; Fig. 14) and probably reflect the sulphur content of the kerogen. Clearly, the depth of the oil shale at Douglas River (320 m) is insufficient to produce this level of thermal maturity, even given a high geothermal gradient for this area of around 30°C/km (GREEN, 1989). This could reflect significant erosion of Tertiary material or be due to past and localised heating of the organic matter. Too little is currently known about the geology of this region of Tasmania to assess which is the more likely of these two alternatives.

The high TOC and HI values confirm that the tasmanite has the potential to generate large amounts of hydrocarbons but importantly, in the east of Tasmania, as shown by the data from Douglas River, its thermal maturity is near the oil window. This result contradicts previous assumptions that the oil shale in Tasmania is too immature to represent a possible petroleum source, although the present day areal extent of mature strata is unknown.

Inferred Environment of Deposition

BANKS (1962), KANSTLER (1980), and CALVER et al. (1984) suggested that *Tasmanites* represents the "cysts" of a planktonic organism living in a restricted environment, generally littoral and associated with reduced salinity due to a high freshwater input. It has been suggested that much of present-day Tasmania was covered during the Late Carboniferous by an ice sheet flowing from the west (BANKS and CLARKE, 1987). At that time Tasmania was positioned in high southern latitudes (ca. 75–80°S; SMITH et al., 1981). As the glaciers retreated, black muds were deposited on the sea floor in front of the ice, and it was in these muds that beds of tasmanite were formed. The occasional presence of fossil brachiopods and starfish in the tasmanite shale indicates a marine setting. Deposition in quiescent shallow to very shallow water is indicated by fine-scale cross lamination, scouring, and lensing-out over very short distances of both the siltstone and *Tasmanites*-rich layers in oil shale from Oonah and by the close association with lenticular sand and well-sorted granule bodies in the Douglas River core. It is suggested that deposition occurred in water depths of 100 m or less (Fig. 3); a nearshore deposition is further suggested by the presence of desmocollinite at Oonah and collinite at Latrobe. The overall fine-grain size of the oil shale–bearing sequence shows that very low current strengths existed at the site of deposition. Lonestones, some of which are demonstrably dropstones (Fig. 4b), may have been transported to the site by shore ice as their shapes are characteristic of fluvial and beach environments with little evidence for transport by glacial ice (DOMACK et al., 1993).

Estimates of sea surface temperature for early Permian Tasmania of −1.8°C (RAO and GREEN, 1982) are close to the present average near the Antarctic ice shelf of −1.9°C. DOMACK et al. (1993) propose that the tasmanite beds record a period of enhanced primary productivity coupled with polar to subpolar glacial marine conditions characterised by very cold waters, seasonal sea ice, and shore-ice rafting. Cold water deposition is consistent with the low diversity of the invertebrate fauna and strongly indicated by the presence of glendonites, pseudomorphs after ikaite (calcium carbonate hexahydrate; $CaCO_3 \cdot 6H_2O$). This mineral is suggested to be an authigenic precipitate, forming at low temperatures from interstitial waters of organic-rich sediments, undergoing microbial degradation and accumulated rapidly in cold bottom-waters (SUESS et al., 1982; SHEARMAN and SMITH, 1985; JANSEN et al., 1987).

It is notable that the sediments where *Tasmanites* is abundant, in the Late Ordovician-Early Silurian of the Sahara, the Devonian of Brazil, the Late Carboniferous-Early Permian

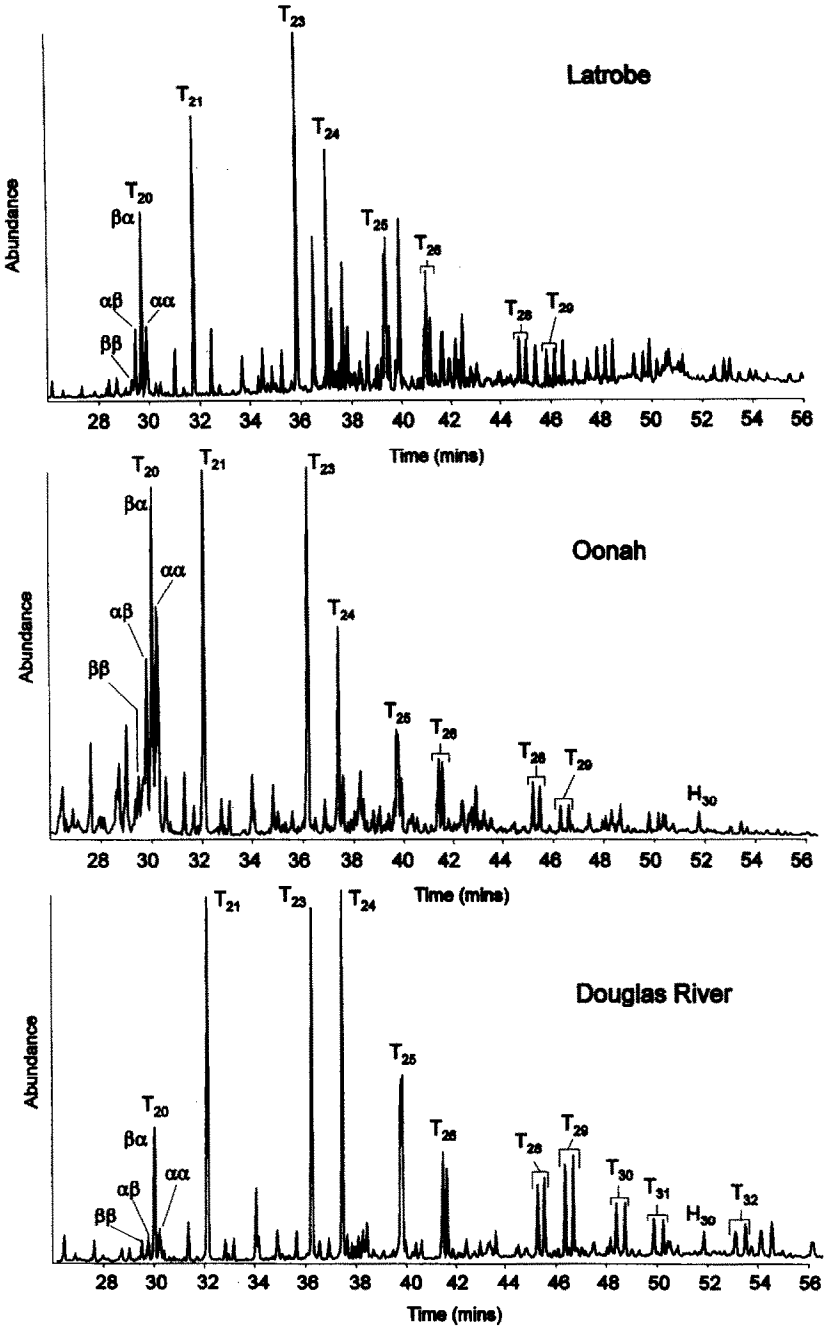

FIG. 11. Extended m/z 191 mass chromatogram for extracts from Latrobe, Oonah, and Douglas River. Numbers refer to carbon number; T = Tricyclics; H = Hopane. Symbols refer to isomerisation at carbons 13 and 14. For example, $\beta\alpha$ refers to 13β(H), 14α(H). Assignments are taken from CHICARELLI et al. (1988). T_{25} structure is shown in Fig. 6.

tasmanite of Tasmania and the *Tasmanites*-rich deposits of the Jurassic/Cretaceous of the Brooks Range, Alaska, all have palaeolatitudes, inferred from palaeomagnetic work, of about 75° (SMITH et al., 1981). Sediments where *Tasmanites* is of low abundance seem to have had a wider latitudinal range. For example, its occurrence at about 10°S in the Devonian of Indiana and Ohio (SMITH et al., 1981) indicates that it was a wide ranging organism comparable to some diatoms and prasinophytes in contemporary oceans.

Pyrite occurs within some fossils, but also separately in the fine siltstone and between fossils. The pyrite is predominantly framboidal and seems to have been an early diagenetic deposit, especially in associated conglomerates. This indicates a reducing environment soon after deposition, which is also supported by the presence of glendonites. Identifiable burrows in the sediments suggest only mild bioturbation and that bottomwaters were depleted in oxygen at the time of deposition which, combined with low temperatures, reduced the rate of oxidation of the organic matter such that little was oxidised prior to burial. Low pristane/phytane ratios are often associated with low-oxygen environments such as the tasmanite (Table 3; DIDYK et al., 1978), although other factors can be

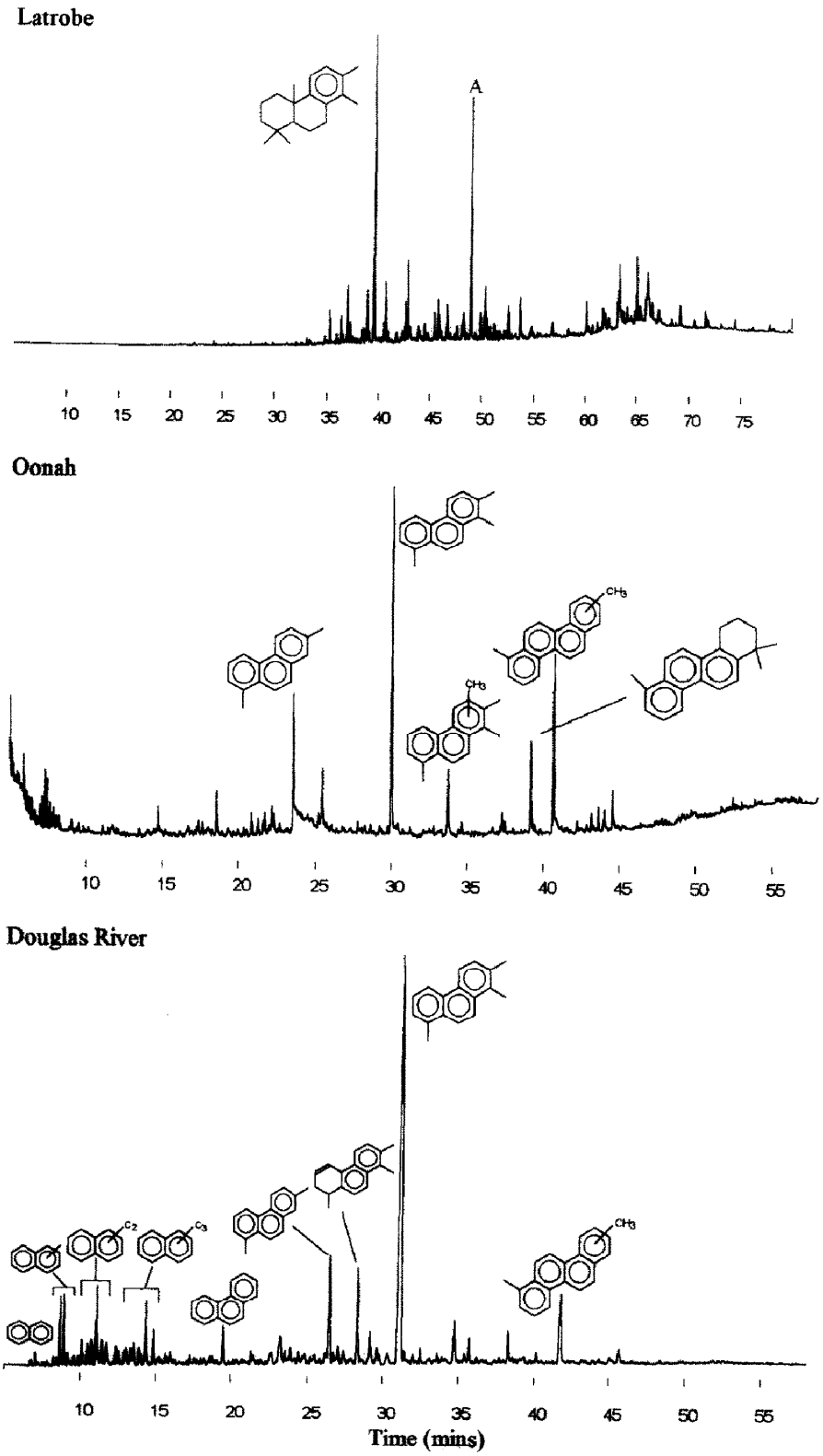

FIG. 12. Gas chromatograms of the aromatic fractions isolated from samples collected at Latrobe, Oonah, and Douglas River. Peak assignments are indicated by structures. Peak A is discussed in the text.

important (TEN HAVEN et al., 1987). In contrast, the siltstone above and below the tasmanite shale which represents deposition in an oxic environment exhibits a relatively high pristane/phytane ratio of 3.1. Our data is consistent with earlier models of tasmanite deposition, suggesting that the sum of the physical properties indicates deposition in a dysaerobic environment with a dissolved oxygen content less than 0.5 ml L^{-1} at the sediment-water interface (ARTHUR et al., 1984).

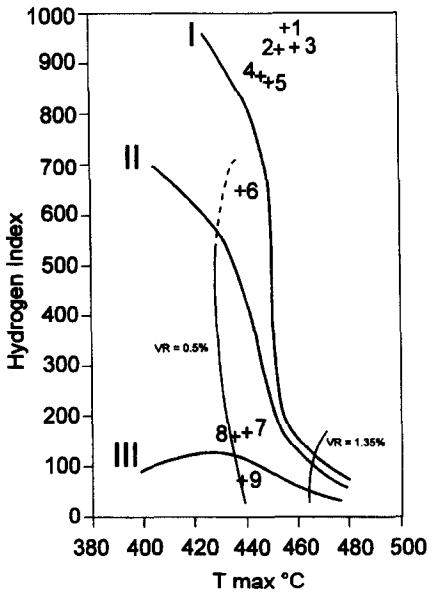

FIG. 13. HI/Tmax plot showing the relative positions of the samples. Note the difference in maturity shown by the algal kerogen and the associated siltstone. The standard 0.5% Vitrinite reflectance contour is shown. 1 = Latrobe, 2 = Oonah upper seam whole rock, 3 = Oonah *Tasmanites* concentrate, 4 = Oonah lower seam *Tasmanites* concentrate, 5 = Oonah lower seam whole rock, 6 = Douglas River whole shale, 7, 8, 9 = Siltstone samples from above and below the oil shale at Oonah.

SIMONEIT et al. (1992, 1993) reported high ^{13}C enrichment for the tricyclic compounds ($\delta^{13}C$ values of -9.9 to -12.2‰) extracted from an immature sample from Latrobe (Fig. 1) which was attributed to bloom conditions prevailing at the time of deposition. Phytoplankton from cold, high latitude waters are typically depleted in ^{13}C due to the elevated P_{CO_2} caused by increased CO_2 solubility at these temperatures (reviewed by SACKETT, 1991). Low atmospheric P_{CO_2} associated with global glaciation (RAU et al., 1991a) in the Early Permian, possibly combined with additional P_{CO_2} drawdown during algal blooms provides a possible explanation for the ^{13}C enrichments of tasmanite kerogen reported here and by SIMONEIT et al. (1993). However RAU et al. (1991b) showed that particulate organic matter associated with sea ice could also be significantly enriched in ^{13}C ($\delta^{13}C$ -16 to -28‰) relative to the seawater. Within the sea-ice the physical isolation from reequilibration with the atmosphere may reduce CO_2 availability and therefore significantly reduce isotopic fractionation. SIMONEIT et al. (1993) reported a tasmanite kerogen with a $\delta^{13}C$ value of -16.6‰ and our samples have $\delta^{13}C$ values of -13 to -11‰ (Fig. 16). Thus, in view of the depositional setting implied by geological evidence we propose that *Tasmanites* in this instance may have occupied an environment very similar to that of present-day sea-ice algae. Thus, by analogy with present-day sea-ice diatom communities, the *Tasmanites* bloomed within the ice as the light intensity increased during the spring. As the ice melted, algae from the bloom were released into the water column and subsequently sedimented. The fine scale laminations and rarity of bioturbation are consistent with a quiescent water column, which may be assisted by persistent ice cover. To test this hypothesis we measured the $\delta^{13}C$ for sea-ice diatoms collected from ice cores taken in Antarctica, during November 1991. These gave a $\delta^{13}C$ value of -7‰ (Fig. 16) which supports this interpretation. Further studies of sea-ice algae from several Antarctic locations have confirmed their ^{13}C enrichment compared to algae isolated from the associated water column (R. E. Summons and P. D. Nichols, unpubl. data). The taxonomic assignment of *Tasmanites* with the Prasinophyceae (Chlorophyta) (WALL, 1962; PARKE, 1966) and the observations of TAPPAN (1980), who suggested that the fossil prasinophytes are a "disaster species," somehow surviving the widespread extinctions of the middle Palaeozoic and, perhaps most importantly, thriving in the absence of other phytoplankton, are all consistent with our model.

Origins of Biomarkers in the Tasmanite Oil Shale

Recently COLLISTER et al. (1992) reported isotopic values for tricyclic compounds in the Green River oil shale which

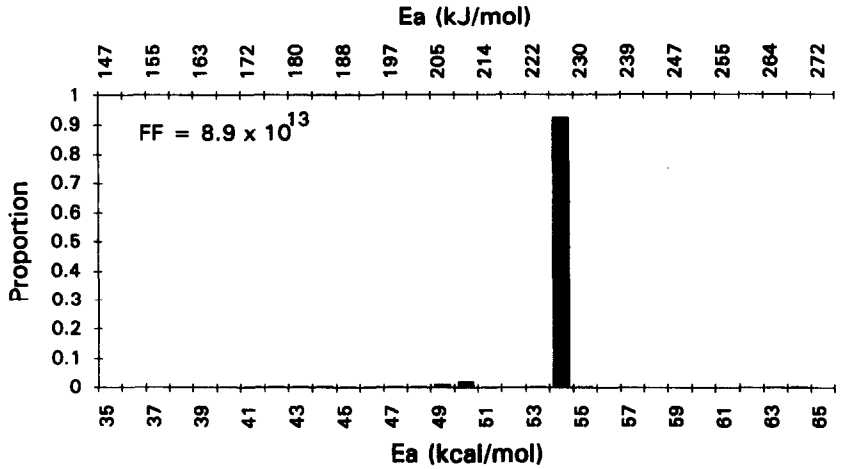

FIG. 14. Plot showing the distribution of activation energies in the Latrobe tasmanite kerogen. FF = Frequency Factor (s^{-1}).

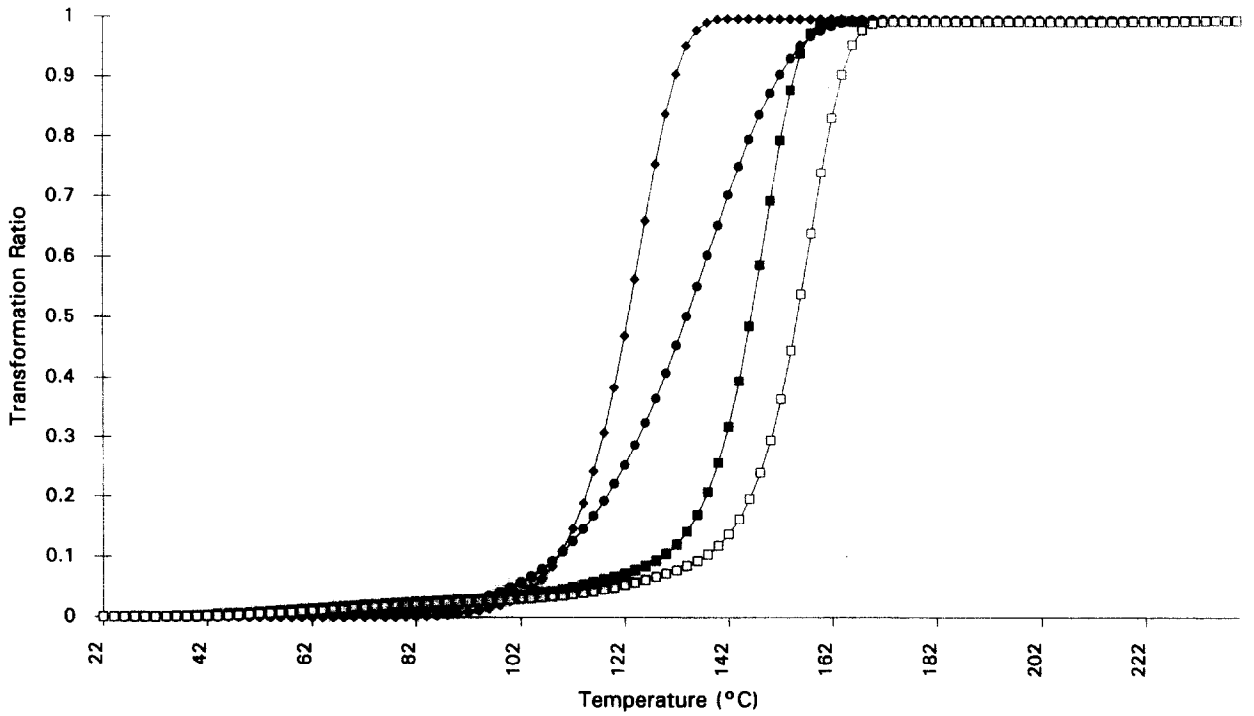

FIG. 15. Simulated maturation of the Latrobe tasmanite kerogen, compared with sterane isomerisation at C_{20}. Sterane activation energies used are those of MACKENZIE and MCKENZIE (1983) — ●— and MARZI and RULLKÖTTER (1992) — ♦—, at 8°C per million years. Tasmanite maturation is shown at 8°C (— □ —) and 2°C (— ■ —) per million years.

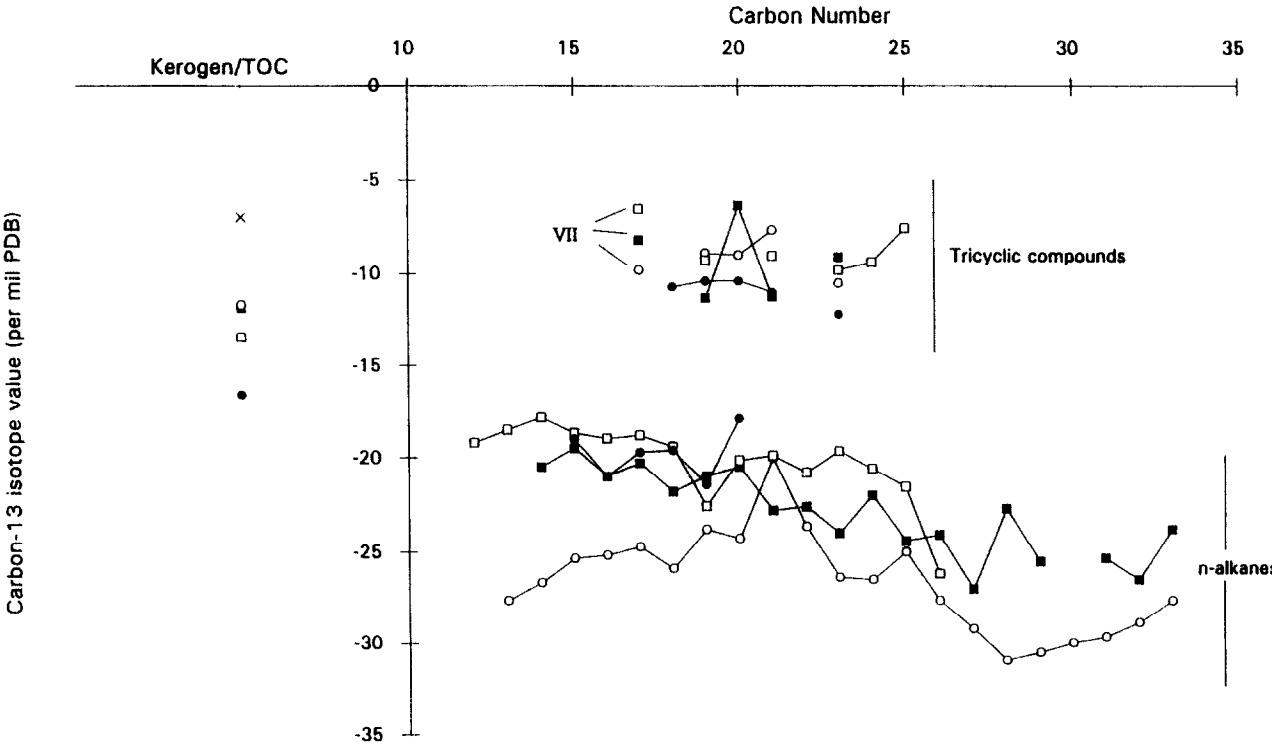

FIG. 16. Plot showing the variation in $\delta^{13}C$ values for kerogen and for *n*-alkanes, tricyclic compounds and aromatic derivatives vs. carbon number. Data from this study are represented as: — ■ — Latrobe; — ○ — Oonah; — □ — Douglas River; and — × — Sea-ice diatoms. Data previously reported by SIMONEIT et al. (1993) are represented as — ● —. Groups of compounds are indicated as *n*-alkanes and cyclic compounds (tricyclic alkanes and aromatic derivatives). Numerals refer to structures in scheme 1, tricyclic alkanes are all of type I. Note that the $\delta^{13}C$ values of kerogen from Latrobe and Oonah are almost identical.

ranged from −33.7 to −27.3‰. This range corresponds to the values generally associated with photoautotrophs, but there was no correlation with the values for β-carotane or steranes in the same samples, indicating different source organisms. The difference between the isotopic values of COLLISTER et al. (1992) and those reported here and by SIMONEIT et al. (1993) may be due to the source organism occupying a different niche in the very different environments of deposition.

The high proportion of preserved organic remains in the tasmanite oil shale, and the dominance of tricyclic compounds in the hydrocarbon fractions, has often led to *Tasmanites* to be proposed as the likely source for these compounds (e.g., VOLKMAN et al., 1989; SIMONEIT et al., 1992, 1993). However, tricyclic compounds have been identified in a wide range of sediments and petroleum from a range of geological ages, and do not appear to be limited to areas of high *Tasmanites* content (see AQUINO NETO et al., 1983), so other sources must be examined. A consideration of $\delta^{13}C$ values of tricyclic compounds in the extracts and pyrolysates of the tasmanite oil shale provides evidence for a source distinct from the accompanying algaenan.

GC-IRMS analysis of tricyclics in previous studies (SIMONEIT et al., 1993) and the present study yielded $\delta^{13}C$ values of −9.9 to −12.2‰ and −6.4 to −11.3‰, respectively, which shows that these compounds are enriched in ^{13}C compared with the corresponding kerogen (Fig. 16). The light and variable isotopic composition for the *n*-alkanes ($\delta^{13}C$ values −18 to −30‰) suggests multiple sources. There is a general trend for ^{13}C depletion in higher *n*-alkane homologues, suggesting a possible contribution from allochthonous bacterial or plant waxes. For the lower *n*-alkane homologues, algal and cyanobacterial sources may become increasingly important.

Closed-system pyrolysis of tasmanite kerogen for 72 h at increasingly higher temperatures showed a number of interesting trends (Table 4). Recovery of bitumen maximised at 68% at 330°C and decreased to 59% at 350°C, probably as a result of the generation of a larger proportion of gas resulting from cracking of liquid hydrocarbons. The composition of the bitumen also changed markedly. At 350°C almost 96% of the bitumen could be recovered from the chromatographic column, as saturates, aromatics, and weakly polar materials. At 300°C and 330°C the recoveries from column chromatography were only 52 and 57%, respectively, indicating that the pyrolysate comprised a major proportion of asphaltic or strongly polar material which bound irreversibly to the silica gel. The proportions of saturates, aromatics, and weakly polar fractions in the material recovered from column chromatography did not change significantly as the pyrolysis temperature increased.

A comparison of GC traces for the C_{10+} saturated hydrocarbons (Fig. 17) shows a low abundance of *n*-alkanes compared to tricyclanes in the extract and the 300°C pyrolysate. At the higher temperatures, *n*-alkanes dominate the GC-FID chromatogram, consistent with flash pyrolysis-GC results which revealed the aliphatic nature of the tasmanite kerogen (C. J. Boreham, unpubl. data). There is also a progression in *n*-alkane generation leading to reduced waxy *n*-alkane contents and lower molecular weight predominance as the temperature increases to 350°C. In the 300°C pyrolysate, the *n*-alkane envelope maximises at C_{18} compared with C_{14} in the 350°C pyrolysate. Evidence for this evolution is also shown by $\delta^{13}C$ analysis of the alkanes (Fig. 18) and comparison with those in the extract. The *n*-alkanes produced at 300°C exhibit an isotopic composition closest to those of the extract with a progression to "heavier" compounds with an increase in pyrolysis temperature. Note that at 350°C the $\delta^{13}C$ values of C_{15}–C_{24} *n*-alkanes are in the range −12 to −15‰, compared with the kerogen at −12‰. The C_{13} and C_{14} *n*-alkanes are now prominent (Fig. 16) and are slightly "heavier" than the starting kerogen at −10 to −11.5‰, although this could be due, in part, to isotopic fractionation on evaporative loss of some of the volatile *n*-alkanes.

The observations from the pyrolysis experiments are consistent with the concept of generation of an asphaltene- and polar-rich material during the initial stages of kerogen conversion (EVANS and FELBECK, 1983), and subsequent cracking of this to lower molecular weight components, including gaseous products. The main information conveyed by the isotope data is, however, that the $\delta^{13}C$ values of the *n*-alkanes produced by kerogen pyrolysis are significantly different from those in the extract of immature tasmanite. Pyrolytically generated *n*-alkanes and *n*-alkylcyclohexanes (data not shown) are isotopically similar to the kerogen consistent with earlier observations (BURWOOD et al., 1988) of a close correlation between ^{13}C contents of sapropellic kerogens and their pyrolysates. Based on experience with other algal-derived kerogens (e.g., GOTH et al., 1988; TEGELAAR et al., 1989; DERENNE et al., 1992; BOREHAM et al., 1994), these compounds are probably derived from an *n*-alkyl based biopolymer, algaenan,

Table 4. Comparison of whole rock extract and kerogen pyrolysate of tasmanite from Latrobe, Tasmania

72 hr Pyrolysis Temp. (°C)	EOM (mg/g TOC)#	C_{12+} Saturates* (%)	Aromatics* (%)	Polars* (%)	Asphaltenes‡ (%)
unheated	51.4	19.0	30.5	38.8	11.7
300	190.8	7.0	13.3	31.3	48.4
330	1019.2	8.5	13.9	39.3	38.3
350	879.1	14.9	42.1	39.7	3.3

TOC (kerogen) = 67.1 %

* Based on pre-chromatography weight

‡ Taken as that fraction not eluting from the chromatographic column

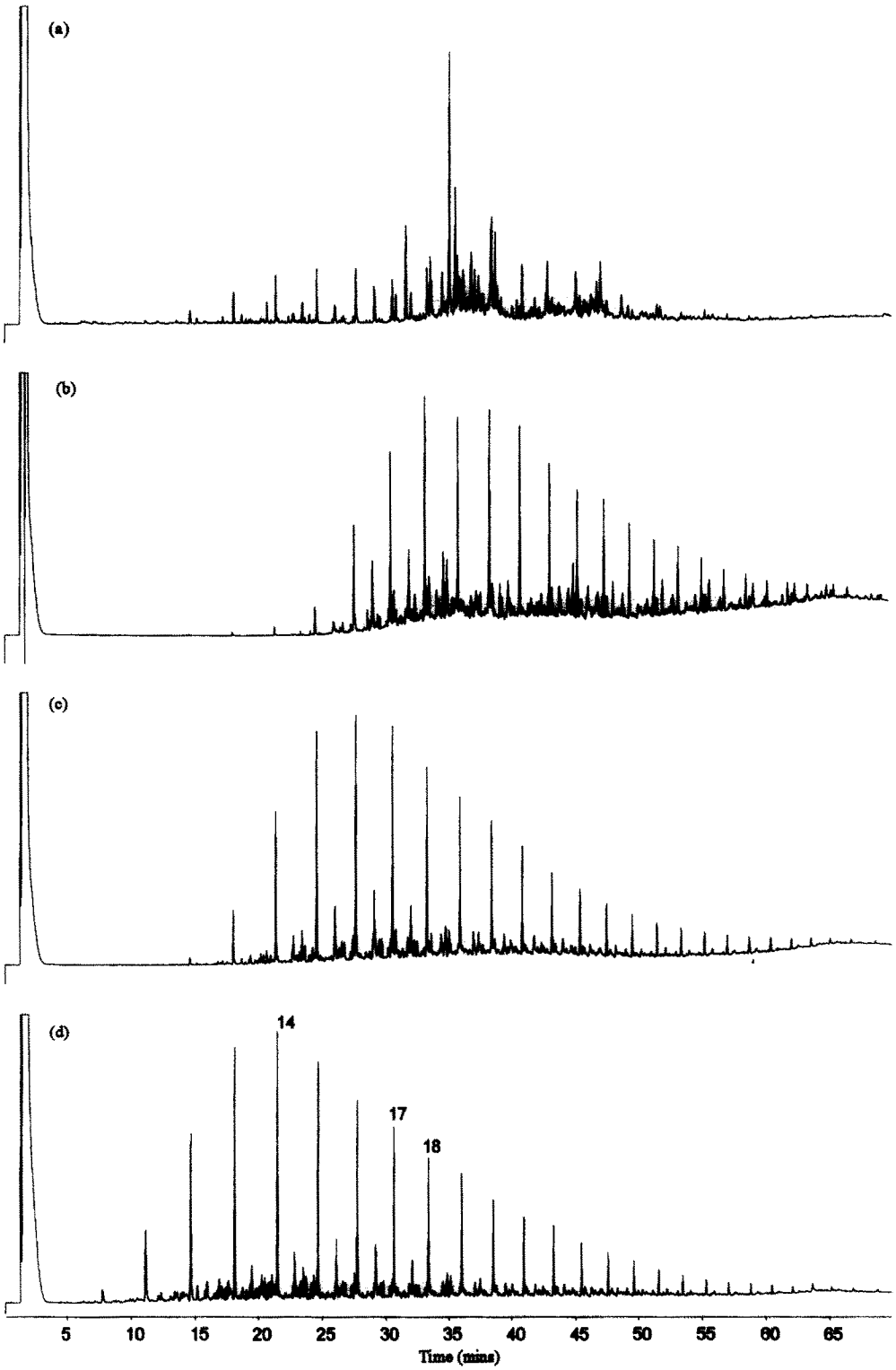

FIG. 17. Gas chromatograms showing the aliphatic hydrocarbons from (a) the original extract and from closed-system pyrolysis of tasmanite kerogen, isolated from a sample collected at Latrobe, at (b) 300°C, (c) 330°C, and (d) 350°C. Note the progressive increase in low molecular weight *n*-alkanes and the relative decrease in tricyclic compounds.

which forms part of the structure of the tasmanite fossils. Indeed, the $\delta^{13}C$ values are constant for the C_{17}–C_{27} *n*-alkanes from the 330°C pyrolysate. Here, yields are high, secondary cracking is minimal and the isotopic value is considered to represent that of the *Tasmanites* algaenan. This is also consistent with the reported aliphatic nature of the preserved organic matter (KJELLSTRÖM, 1968).

Saturated tricyclic alkanes did not appear to be generated during the 330 and 350°C pyrolyses where the *n*-alkanes were mostly produced. Their abundance relative to the *n*-alkanes

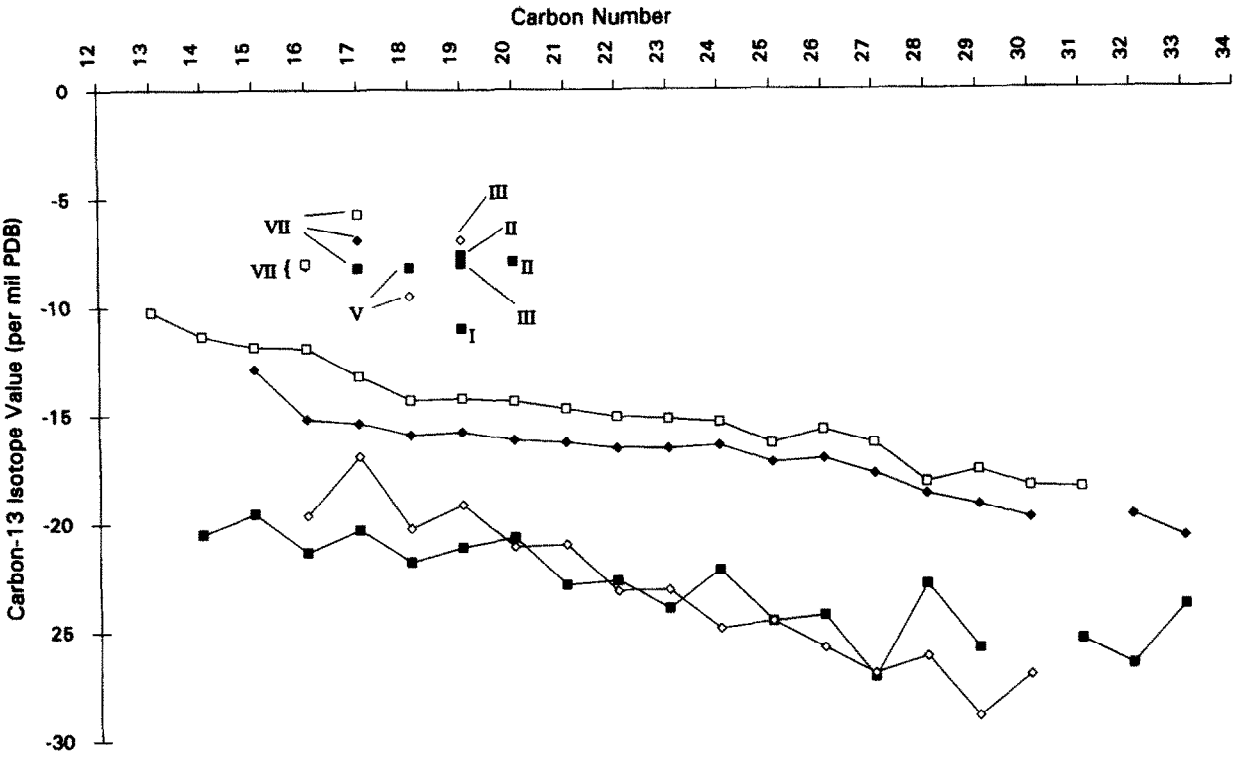

FIG. 18. Chart showing the $\delta^{13}C$ values of (a) *n*-alkanes liberated by pyrolysis at 300°C — ◇ —, 330°C — ♦ — and 350°C — □ — of tasmanite kerogen from Latrobe (AGSO sample # 1995), compared with the original extract — ■ — (b) tricyclic hydrocarbons (structures I–VII in scheme 1) from Latrobe (extract and pyrolysate, symbols as in (a)).

decreased as the temperature increased. Caution should be exercised however. Tricyclic hydrocarbons may have been converted to aromatics at higher pyrolysis temperatures. Furthermore, the composition of the aromatic fractions generated in the pyrolysis experiments became much simpler with increasing temperature and at 350°C was dominated by 1,7-dimethylphenanthrene and 1,2,8-trimethylphenanthrene with $\delta^{13}C$ values of −7.9 and −5.7‰, respectively, which are within the range for tricyclic compounds in the tasmanite extracts of different maturities (Fig. 16). The isotopic similarity in the tricyclic hydrocarbons from pyrolysis and tasmanite extracts (Scheme 1 and Fig. 18) suggest that they are almost certainly derived from the same precursors. A proposed genetic relationship between the tricyclic hydrocarbons is shown in Scheme 1. It is uncertain at present whether this process is mediated by bacteria or by heating in the natural environment (LOHMANN, 1988; FREEMAN, 1991; FREEMAN et al., 1994). Certainly, the latter process is indicated by the bias towards the fully aromatised tricyclics in both the pyrolysates and the higher maturity Oonah and Douglas River extracts. Peak A in Fig. 12 has previously been assigned to a tetracyclic monoaromatic des-A-gammacerane (SIMONEIT et al., 1993). However, preliminary NMR data on this compound suggests that it is not a des-A-oleanane or des-A-gammacerane (BOREHAM and WILKINS, 1994) and the isotopic similarity between it (−8.5‰) and the tricyclic compounds suggests a common source.

The isotopic dissimilarity of the tricyclic hydrocarbons (mean −8‰) to the kerogen and kerogen-derived *n*-alkanes suggests a source distinct from the *Tasmanites* themselves.

Interestingly, the difference in kerogen $\delta^{13}C$ data in this study with that of SIMONEIT et al. (1993) is matched by differences of a similar magnitude in the tricyclic compounds, aromatic derivatives, and *n*-alkanes in the extracts. This, in conjunction with the previously noted differences in sterane and hopane observations, suggests that there were fluctuations in the source and depositional environment of organic matter within the oil shale seam which affected both biomarker distributions and their ^{13}C isotopic values.

CONCLUSIONS

This study represents the first organic geochemical comparison of thermally mature and immature tasmanite oil shale samples in conjunction with a detailed geological evaluation of the sedimentary setting.

1) This study has shown, for the first time, that at least some deposits of the tasmanite shale in Tasmania are near the "oil window."
2) Geological, isotopic, and biomarker analysis indicates that *Tasmanites* thrived in an environment of ice cover and bloomed in conditions analogous to those experienced by present-day sea-ice diatoms. The algal cells were subsequently deposited in sediments overlain with oxygen-depleted waters, induced by restricted water movement.
3) Closed-system pyrolysis suggests that there is little correlation between the temperature profiles for production of *n*-alkanes and the tricyclic compounds from the kerogen precursors. The *n*-alkanes are mainly derived from thermal cracking of algal aliphatic biopolymer whereas the tricyclic

alkanes and aromatic hydrocarbons are generated earlier, possibly from a different source.

Acknowledgments—Dr. S. J. Rowland, University of Plymouth, is thanked for kindly supplying a sample of authentic 1,2,8-trimethylphenanthrene. Peter Baillie (Tasmanian Department of Mines) provided the Latrobe sample (BMR #1995) and Janet Hope carried out closed-system pyrolysis on this sample. We would like to thank Dr. Peter Nichols (CSIRO) for providing the sea-ice diatom sample and Malcolm Bendall for information about the Douglas River core. ATR thanks the CSIRO Institute of Natural Resources and Environment for a post-doctoral fellowship. Andrew Murray and Dr. Clinton Foster (AGSO) provided valuable reviews of early versions of the manuscript and AM is thanked for providing the data for Fig. 15. We are grateful to Professor B. R. T. Simoneit for a preprint of unpublished data and to Dr. J. W. De Leeuw, Dr. H. L. ten Haven, Dr. J. M. Moldowan, and Dr. M. Radke for very helpful reviews of the manuscript. RES and CJB publish with permission of the Director, AGSO.

Editorial handling: J. T. Senftle

REFERENCES

AQUINO NETO F. R., RESTLE A., CONNAN J., ALBRECHT P., and OURISSON G. (1982) Novel tricyclic terpanes (C_{19}, C_{20}) in sediments and petroleums. *Tetrahedron Lett.* **23**, 2027–2030.

AQUINO NETO F. R., TRENDEL J. M., RESTLE A., CONNAN J., and ALBRECHT P. (1983) Occurrence and formation of tricyclic and tetracyclic terpanes in sediments and petroleums. In *Advances in Organic Geochemistry 1981* (ed. M. BJORØY et al.), pp. 659–667. Wiley.

AQUINO NETO F. R., TRIGÜIS D. A., AZEVEDO D. A., RODRIGUES R., and SIMONEIT B. R. T. (1992) Organic geochemistry of geographically unrelated *Tasmanites*. *Org. Geochem.* **18**, 791–803.

ARTHUR M. A., DEAN W. E., and STOW D. A. V. (1984) Models for the deposition of Mesozoic-Cenezoic fine-grained organic-rich sediment in the deep sea. In *Fine-Grained Sediments: Deep-Water Processes and Facies* (ed. D. A. V. STOW and D. J. W. PIPER); *Geol. Soc. Special Publication*, pp. 527–560.

AZEVEDO D. A., AQUINO NETO F. R., and SIMONEIT B. R. T. (1990) Mass spectrometric characteristics of a novel series of ring-C monoaromatic tricyclic terpanes found in Tasmanian tasmanite. *Org. Mass Spectrom.* **25**, 475–480.

AZEVEDO D. A., AQUINO NETO F. R., SIMONEIT B. R. T., and PINTO A. C. (1992) Novel series of tricyclic aromatic terpanes characterized in Tasmanian tasmanite. *Org. Geochem.* **18**, 9–16.

BANKS M. R. (1962) Permian (Tasmania). *J. Geol. Soc. Australia* **9**, 189–216.

BANKS M. R. and CLARKE M. J. (1987) Changes in the geography of the Tasmania Basin in the late Paleozoic. In *Gondwana Six: Stratigraphy, Sedimentology and Paleontology* (ed. G. D. MCKENZIE); *Amer. Geophys. Union Geophys. Monograph 41*, pp. 1–14.

BENDALL M. R., VOLKMAN J. K., LEAMAN D. E., and BURRETT C. F. (1991) Recent developments in exploration for oil in Tasmania. *APEA J.* part 1, **31**, 74–84.

BOALCH G. T. and GUY-OHLSON D. (1992) *Tasmanites*, the correct name for *Pachysphaera* (Prasinophyceae, *Pterospermataceae*). *Taxon* **41**, 529–531.

BORDENAVE M. L., ESPITALIÉ J., LEPLAT P., OUDIN J. L., and VANDENBROUCKE M. (1993) Screening Techniques for Source Rock Evaluation. In *Applied Petroleum Geochemistry* (ed. M. L. BORDENAVE), Chap. II-2, pp. 217–278. Editions Tecnip.

BOREHAM C. J. and WILKINS, A. L. (1994) Structure and origin of the two major monoaromatic hydrocarbons in a tasmanite oil shale from Tasmania, Australia. *Tetrahedron* (submitted).

BOREHAM C. J., CRICK I. H., and POWELL T. G. (1988) Alternative calibration of the Methylphenanthrene Index against vitrinite reflectance: Application to maturity measurements on oils and sediments. *Org. Geochem.* **12**, 289–294.

BOREHAM C. J., SUMMONS R. E., ROKSANDIC Z., DOWLING L. M., and HUTTON A. C. (1994) Chemical, molecular and isotopic differentiation of organic facies in the tertiary lacustrine Duaringa oil shale deposit, Queensland, Australia. *Org. Geochem.* **21**, 685–712.

BURLINGAME A. L., WSZOLEK P. C., and SIMONEIT B. R. T. (1969) The fatty acid content of tasmanites. In *Advances in Organic Geochemistry 1968* (ed. P. A. SCHENCK and I. HEVENAAR), pp. 131–155. Pergamon-Vieweg.

BURWOOD R., DROZD R. J., HALPERN H. I., and SEDIVY R. A. (1988) Carbon isotopic variations of kerogen pyrolysates. *Org. Geochem.* **12**, 195–205.

CALVER C. R., CLARKE M. J., and TRUSWELL E. M. (1984) The stratigraphy of a late Palaeozoic bore hole section at Douglas River, eastern Tasmania: a synthesis of marine macro-invertebrate and palynological data. *Pap. Proc. R. Soc. Tasm.* **118**, 137–161.

CHICARELLI M. I., AQUINO NETO F. R., and ALBRECHT P. (1988) Occurrence of four stereoisomeric tricyclic terpane series in immature Brazilian shales. *Geochim. Cosmochim. Acta* **52**, 1955–1959.

CLARKE M. J. (1989) Lower Parmeener Supergroup. In *Geology and Mineral Resources of Tasmania* (ed. C. F. BURRETT and E. L. MARTIN); *Geol. Soc. Australia, Special Publication 15*, Chap. 8, pp. 295–309.

CLARKE M. J. (1992) *Hellyerian and Tamarian (Late Carboniferous-Lower Permian) Invertebrate Faunas from Tasmania: Tasm. Geol. Surv. Bull. 69.*

CLARKE M. J. and BANKS M. R. (1975) The stratigraphy of the Lower (Permo-Carboniferous) parts of the Parmeener super-group, Tasmania. In *Gondwana Geology* (ed. K. S. W. CAMPBELL), pp. 453–467. A.N.U. Press.

CLARKE M. J. and FARMER N. (1976) Biostratigraphic nomenclature for late Palaeozoic rocks in Tasmania. *Pap. Proc. R. Soc. Tasm.* **110**, 91–109.

COLLISTER J. W., SUMMONS R. E., LICHTFOUSE E., and HAYES J. M. (1992) An isotopic biogeochemical study of the Green River oil shale. *Org. Geochem.* **19**, 265–276.

DERENNE S., LE BERRE F., LARGEAU C., HATCHER P., CONNAN J., and RAYNAUD J. F. (1992) Formation of ultralaminae in marine kerogens via selective preservation of thin resistant outer walls of microalgae. *Org. Geochem.* **19**, 345–350.

DIDYK B. M., SIMONEIT B. R. T., BRASSELL S. C., and EGLINTON G. (1978) Organic geochemical indicators of palaeoenvironmental conditions of sedimentation. *Nature* (London) **272**, 216–222.

DOMACK E. W., BURKLEY L. A., DOMACK C. R., and BANKS M. R. (1993) Facies analysis of glacial marine pebbly mudstones in the Tasmania Basin: Implications for regional paleoclimates during the late Paleozoic. In *Gondwana Eight: Proceedings of the Eighth Gondwana Symposium* (ed. R. H. FINDLAY et al.), pp. 471–484. Balkema.

EVANS R. J. and FELBECK G. T., JR. (1983) High temperature simulation of petroleum formation—1. The pyrolysis of Green River shale. *Org. Geochem.* **4**, 135–144.

FOSTER C. B. and WATERHOUSE J. B. (1988) The Granulatisporites confluens Oppel-zone and Early Permian marine faunas from the Grant Formation on the Barbwire Terrace, Canning Basin, Western Australia. *Australian J. Earth Sci.* **35**, 135–157.

FREEMAN K. H. (1991) The carbon isotopic composition of individual compounds from ancient and modern depositional environments. Ph.D. thesis, Indiana University.

FREEMAN K. H., BOREHAM C. J., SUMMONS R. E., and HAYES J. M. (1994) The effect of aromatisation on the isotopic compositions of hydrocarbons during early diagenesis. *Org. Geochem.* (in press).

GOTH K., DE LEEUW J. W., PÜTTMANN W., and TEGELAAR E. W. (1988) Origin of Messel Oil Shale kerogen. *Nature* (London) **336**, 759–761.

GOULD C. (1861) Resinous shales (Dysodile at Latrobe). *Tasm. House of Assembly Pap.* **8.**

GREEN D. C. (1989) Heat flow and heat production in Tasmania. In *Geology and Mineral Resources of Tasmania* (ed. C. F. BURRETT and E. L. MARTIN); *Geol. Soc. Australia, Special Publication 15*, Chap. 13, pp. 461–463.

GUY-OHLSON D. (1988) Developmental stages in the life cycle of Mesozoic *Tasmanites*. *Bot. Mar.* **31**, 447–456.

GUY-OHLSON D. and BOALCH G. T. (1992) Comparative morphology of the genus *Tasmanites* (Pterospermales, Chlorophyta). *Phycologia* **31**, 523–528.

HARLAND W. B., ARMSTRONG R. L., COX A. V., CRAIG L. E., SMITH A. G., and SMITH D. G. (1990) *A Geological Timescale 1989*. Cambridge Univ. Press.

HAYES J. M., FREEMAN K. H., POPP B. N., and HOHAM C. H. (1990) Compound-specific isotope analysis: a novel tool for reconstruction of ancient biogeochemical processes. In *Advances in Organic Geochemistry 1989* (ed. B. DURAND and F. BEHAR), pp. 1115–1128. Pergamon Press.

JAMES C., GEPP H. W., AIKENHEAD A., SCOTT J. B., NYE P. B., PURVES S. S. B., CHAMBERS C. O., JUDE T. M., and REES H. W. (1932) *Report of the Tasmanian Shale Oil Investigation Committee*. Tasmania Department of Mines, Geological Survey, Mineral Resources, No. 8, vol. II. (Reprinted 1950).

JANSEN J. H. F., WOENSDREGT C. F., KOOISTRA M. J., and VAN DER GAAST S. J. (1987) Ikaite pseudomorphs in the Zaire deep-sea fan: an intermediate between calcite and porous calcite. *Geology* **15**, 245–248.

KANTSLER A. J. (1980) Aspects of organic petrology with particular reference to the exinite group of macerals. In *Oil Shale Petrology Workshop, Wollongong, 1980* (ed. A. C. COOK and A. J. KANSTLER), pp. 16–41. Keiraville Kopiers.

KJELLSTRÖM G. (1968) Remarks on the chemistry and ultrastructure of the cell wall of some Palaeozoic Leiospheres. *Geolog. Förenin. Stockh. Förhandlin.* **90**, 221–228.

LOHMANN F. (1988) Aromatistations microbiennes de triterpenes vegetaux. Ph.D. dissertation, L'Université Louis Pasteur de Strasbourg.

MACKENZIE A. S. and MCKENZIE D. P. (1983) Aromatization and isomerization of hydrocarbons in sedimentary basins formed by extension. *Geol. Mag.* **120**, 417–470.

MARZI R. and RULLKÖTTER J. (1992) Qualitative and quantitative evolution and kinetics of biological marker transformations—laboratory experiments and application to the Michigan Basin. In *Biological Markers in Sediments and Petroleum* (ed. J. M. MOLDOWAN et al.), pp. 18–41. Prentice-Hall.

MILLIGAN J. (1852) Report on the coal said to have been found at the Don River, and upon the west bank of the Tamar River, in Tasmania. *Pap. Proc. R. Soc. V.D.L.* **II**, 90–106.

MOLDOWAN J. M., FAGO F. J., LEE C. Y., JACOBSON S. R., WATT D. S., SLOUGUI N. E., JEGANATHAN A., and YOUNG D. C. (1990) Sedimentary 24-*n*-propylcholestanes, molecular fossils diagnostic of marine algae. *Science* **247**, 309–312.

NEWTON E. T. (1875) On 'tasmanite' and Australian 'white coal'. *Geol. Mag.* **12**, 337–342.

OSTENFELD C. H. (1899) Pachysphaera. In *Iagttagelser over overfladevandets temperatur, saltholdighed og plankton pa islandske og gronlandske skibsroyteri 1898*. Bianco Lunos Hof-Bogtrykkeri.

PARKE M. (1966) The genus *Pachysphaera* (Prasinophyceae). In *Some Contemporary Studies in Marine Science* (ed. H. BARNES), pp. 555–563. Allen and Unwin.

PARKE M. and HARTOG-ADAMS I. (1965) Three species of *Halosphaera*. *J. Mar. Biol. Ass. U.K.* **45**, 537–557.

PARKE M., BOALCH G. T., JOWETT R., and HARBOUR D. S. (1978) The genus *Pterosperma* (Prasinophyceae): Species with a single equatorial ala. *J. Mar. Biol. Ass. U.K.* **58**, 239–276.

PETERS K. E. and MOLDOWAN J. M. (1993) *The Biomarker Guide. Interpreting Molecular Fossils in Petroleum and Ancient Sediments*. Prentice-Hall.

PHILP R. P., GILBERT T. D., and RUSSELL N. J. (1982) Characterization by pyrolysis-gas chromatography-mass spectrometry of the insoluble organic residues derived from the hydrogenation of *Tasmanites* sp. oil shale. *Fuel* **61**, 221–226.

RADKE M., WELTE D. H., and WILLSCH H. (1986) Maturity parameters based on aromatic hydrocarbons: influence of organic matter type. In *Advances in Organic Geochemistry 1985. Part I: Petroleum Geochemistry* (ed. D. LEYTHAEUSER and J. RULLKÖTTER), pp. 51–64. Pergamon Press.

RAO C. P. and GREEN D. C. (1982) Oxygen and carbon isotopes of Early Permian cold-water carbonates, Tasmania, Australia. *J. Sediment. Petrol.* **52**, 1111–1125.

RAU G. H., FROELICH P. N., TAKAHASHI T., and DES MARAIS D. J. (1991a) Does sedimentary organic $\delta^{13}C$ record variations in Quaternary ocean [CO_2(aq)]?. *Paleoceanogr.* **6**, 335–347.

RAU G. H., SULLIVAN C. W., and GORDON L. I. (1991b) $\delta^{13}C$ and $\delta^{15}N$ variations in Weddell Sea particulate organic matter. *Mar. Chem.* **35**, 355–369.

REVILL A. T., VOLKMAN J. K., O'LEARY T., and SUMMONS R. E. (1993) Aromatic hydrocarbon biomarkers in tasmanite oil shales from Tasmania, Australia. In *Organic Geochemistry: Poster Sessions from the 16th Intl. Mtg. on Organic Geochemistry, Stavanger 1993* (ed. K. ØYGARD), pp. 3–6. Falch Hurtigtrykk.

SACKETT W. M. (1991) A history of the $\delta^{13}C$ composition of oceanic plankton. *Mar. Chem.* **34**, 153–156.

SHEARMAN D. and SMITH A. J. (1985) Ikaite, the parent material of jarrowite-type pseudomorphs. *Proc. Geol. Assoc.* **96**, 305–314.

SIMONEIT B. R. T. and BURLINGAME A. L. (1973) Carboxylic acids derived from Tasmanian tasmanite by extractions and kerogen oxidations. *Geochim. Cosmochim. Acta* **37**, 595–610.

SIMONEIT B. R. T., LEIF R. N., AQUINO NETO F. R., AZEVEDO A. D., PINTO A. C., and ALBRECHT P. (1990) On the presence of tricyclic terpane hydrocarbons in Permian tasmanite algae. *Naturwissenschaften* **77**, 380–383.

SIMONEIT B. R. T., SCHOELL M., and AQUINO NETO F. R. (1992) Sources of biomarkers in Permian tasmanite based on carbon isotope compositions of individual compounds. Abstract of a presentation at Amer. Chem. Soc. mtg., San Francisco.

SIMONEIT B. R. T., SCHOELL M., DIAS R. F., and AQUINO NETO F. R. (1993) Unusual carbon isotope compositions of biomarker hydrocarbons in a Permian tasmanite. *Geochim. Cosmochim. Acta* **57**, 4205–4211.

SMITH A. G., HURLEY A. M., and BRIDEN J. C. (1981) *Phanerozoic Palaeocontinental World Maps*. Cambridge Univ. Press.

SUESS E., BALZER W., HESSE K.-F., MÜLLER P. J., UNGERER C. A., and WEFER G. (1982) Calcium carbonate hexahydrate from organic-rich sediments of the Antarctic shelf: precursors of glendonites. *Science* **216**, 1128–1131.

TAPPAN H. (1980) *The Paleobiology of Plant Protists*. Freeman.

TEGELAAR E. W., DE LEEUW J. W., DERENNE S., and LARGEAU C. (1989) A reappraisal of kerogen formation. *Geochim. Cosmochim. Acta* **53**, 3103–3106.

TEN HAVEN H. L., DE LEEUW J. W., RULLKÖTTER J., and SINNINGHE DAMSTÉ J. S. (1987) Restricted use of the pristane/phytane ratio as a palaeoenvironmental indicator. *Nature* (London) **330**, 641–643.

TISSOT B. P. and WELTE D. H. (1984) *Petroleum Formation and Occurrence*. Springer-Verlag.

TISSOT B. P., PELET R., and UNGERER P. (1987) Thermal history of sedimentary basins, maturation indices, and kinetics of oil and gas generation. *AAPG Bull.* **71**, 1445–1466.

TRENDEL J.-M. (1985) Degradation de triterpenes dans les sediments: aspects photochemique et microbiologiques. Ph.D. dissertation, L'Université Louis Pasteur de Strasbourg.

TRENDEL J.-M., LOHMANN F., KINTZINGER J. P., and ALBRECHT P. (1989) Identification of des-A-triterpenoid hydrocarbons occurring in surface sediments. *Tetrahedron* **45**, 4457–4470.

TRUSWELL E. M. (1978) *Palynology of the Permo-Carboniferous in Tasmania: An Interim Report; Tas. Geol. Survey Bull. No. 56*. Dept. Mines, Hobart, Tasmania.

TWELVETREES W. H. (1917) The search for petroleum in Tasmania. *Tasm. Mines Dept. Circ.* **2**, 1–18.

VOLKMAN J. K., EVERITT D. A., and ALLEN D. I. (1986) Some analyses of lipid classes in marine organisms, sediments and seawater using thin-layer chromatography-flame ionisation detection. *J. Chromatogr.* **356**, 147–162.

VOLKMAN J. K., BANKS M. R., DENWER K., and AQUINO NETO F. R. (1989) Biomarker composition and depositional setting of tasmanite oil shale. Poster presentation. 14th Intl. Mtg. on Organic Geochemistry, Paris, France.

VOLKMAN J. K., O'LEARY T., SUMMONS R. E., and BENDALL M. R. (1992) Biomarker composition of some asphaltic coastal bitumens from Tasmania, Australia. *Org. Geochem.* **18**, 669–682.

WALL D. (1962) Evidence from recent plankton regarding the biological affinities of *Tasmanites* Newton 1875 and *Leiospaeridea* Eisenack 1958. *Geol. Mag.* **94**, 353–362.

WOLFF G. A., TRENDEL J.-M., and ALBRECHT P. (1989) Novel monoaromatic triterpenoid hydrocarbons occurring in sediments. *Tetrahedron* **45**, 6721–6728.

APPENDIX

Scheme 1

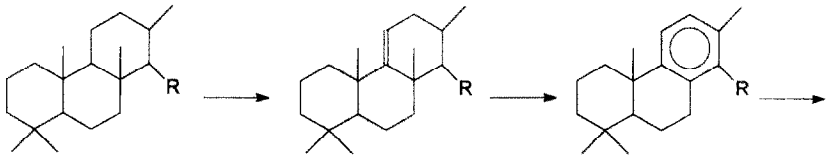

I

$\delta^{13}C$ = -11 ‰ to -6.4 ‰
mean = -8 ‰

II

$C_{19:4}$ -7.6 ‰
$C_{20:4}$ -7.2 ‰

III

$C_{19:6}$ -8.6 ‰ to -7.0 ‰

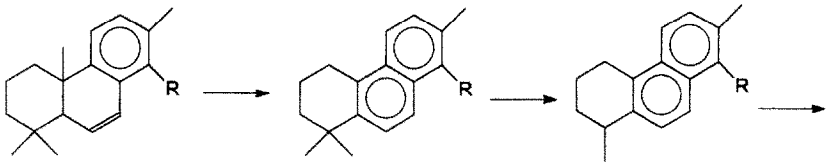

IV

$C_{19:7}$

V

$C_{18:8}$ -9.5 ‰ to -8.1 ‰

VI

$C_{17:9}$ -8.1 ‰

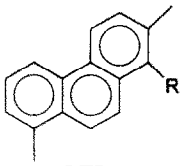

VII

$C_{16:10}$ -8.3 ‰ to -7.6 ‰
$C_{17:10}$ -9.8 ‰ to -6.0 ‰

Proposed general scheme for tricyclic compound aromatisation. R = H or alkyl chain, Cn:x, n = carbon number, x = rings + double bonds. Compound IV could be identified but no isotopic data could be obtained. Compounds I, III and V-VII had mass spectra comparable to published data. For type II ($C_{19:4}$) M^+ 260 (27 %), 245 (100), 189 (8), 175 (29), 163 (15), 149 (67), 119 (21); type IV ($C_{19:7}$) M^+ 254 (35), 239 (45), 183 (42), 169 (100).